5 Noninvasive Quantification of Foliar Pigments
Principles and Implementation

Anatoly Gitelson and Alexei Solovchenko

CONTENTS

5.1 INTRODUCTION

Pigments are central to the functioning of photosynthetic apparatus and hence for all vital functions of plants. Green chlorophylls (Chl), represented by Chl *a* and *b*, the primary photosynthetic pigments, absorb light energy and eventually convert it into chemical energy in the form of electron flow [1–3]. Yellow-to-orange carotenoids (Car) are the accessory pigments that augment Chl in light absorption and serve the indispensable function of protection of the photosynthetic apparatus from photooxidative damage, mostly via elimination of reactive oxygen species and thermal dissipation of excessively absorbed light energy via operation of the xanthophyll cycle [1,4,5]. Foliar Car are usually represented by carotenes, mostly β-carotene, and xanthophylls—lutein, zeaxanthin, violaxanthin, antheraxanthin, and neoxanthin [6]. The retention of carotenoids in the progress of chlorophyll breakdown has been suggested as a mechanism of photoprotection during leaf senescence [7,8]. Changes in leaf carotenoid content and its proportion to chlorophyll are widely used for diagnosing the physiological state of plants during development, senescence, acclimation, and adaptation to different environments and stresses [9].

Another widespread pigment group, flavonoids include red-colored anthocyanins (AnCs) and pale-yellow flavonols (Flv) important for optical shielding of plant tissues in the green and UV-to-blue regions of the spectrum, respectively [10–12]. In leaves, they localize in vacuoles of epidermal cells or those just below the adaxial epidermis, but occasionally also in the cells of abaxial epidermis, palisade, and spongy mesophyll [13]. The induction of AnC biosynthesis occurs as a result of deficiencies in nitrogen and phosphorus, wounding, pathogen infection, desiccation, low temperature, UV irradiation, and so on, so it is generally accepted that AnCs fulfill important physiological functions by being involved in adaptation to numerous stresses and environmental strain reduction [14–16]. Some lines of evidence suggest that the protective effects of anthocyanins

are related to their ability, via screening and/or internal light trapping, to reduce the amount of excessive solar radiation reaching photosynthetic apparati [11,15].

There are also more exotic pigment groups like betalains [17,18] and secondary keto-carotenoids possessing optical properties very similar to those of AnC [7]. Apart from their photosynthetic and photoprotective functions, the pigments serve a plethora of other important functions like attraction of pollinators.

Since pigments are important for the function of plant organisms, their biosynthesis and catabolism are tightly regulated, making them informative markers of plant physiological condition and, ultimately, plant productivity. There are several reasons leaf pigmentation is important from an applied perspective to both land managers and ecophysiologists [19]. First, the amount of solar radiation absorbed by a leaf is largely a function of the foliar contents of photosynthetic pigments; therefore, Chl content in many situations determines the photosynthetic potential and hence primary production [20–22]. Second, much of leaf nitrogen is represented by and correlates with Chl, so quantifying Chl gives an indirect but precise measure of nitrogen nutrition status [22,23]. Third, plant stresses are manifested by directed and specific changes in pigment composition. Thus, the content of Car generally increases and that of Chl decreases under stress and during senescence [9]. The relative contents of photosynthetic pigments reflect the effects of abiotic factors such as light; for example, sun leaves have a higher Chl *a*/Chl *b* ratio [24] and so quantifying these proportions can provide important information about relationships between plants and their environment.

Traditional methods of "wet" pigment analysis (extraction with subsequent spectrophotometry or high-pressure liquid chromatography (HPLC) are destructive and do not permit repeated measurement on the same samples, so it is impossible to follow the changes of vegetation condition in time. These techniques are time consuming and expensive, thus making assessment of the vegetation state on the landscape and ecosystem scales impractical. An alternative solution for leaf pigment analysis is represented by nondestructive optical methods. Monitoring plant physiological status via measuring leaf optical properties such as absorbance and/or reflectance possesses a number of distinct advantages over traditional destructive approaches. The most important ones are simplicity, sensitivity, reliability, and a high throughput, translating into their applicability on a large spatial scale and saving a lot of labor [25].

Developing and implementing methods for quantification of pigment content and composition via nondestructive measurement of optical properties would provide a deeper insight into the physiology of photosynthetic apparatus (regulation of light harvesting and photochemical utilization, balance of photoprotection and photodamage) under favorable conditions and under stress [20,25,26].

The absorption of light by plant pigments allows tracking their content-affecting spectra of optical properties, absorbance, transmittance, and reflectance. Accurate estimation of pigment content using absorbance (α) and reflectance (ρ) spectra requires close linear relationships with the content of the specific pigment of interest. Importantly, these relationships should have a minimal effect of other pigments. Since the absorption bands of the pigments often overlap, it is a challenging problem; hence, development of quantitative measures of α and ρ response to specific pigment content is a prerequisite for assessment of the potential for nondestructive technologies based either on α or ρ spectroscopy.

Kubelka-Munk theory [27,28] laid a basis for reflectance spectroscopy, suggesting that the relationship between remission function, which in reality is reciprocal reflectance, ρ^{-1} [29], is related to the ratio of absorption to scattering coefficients. However, this assumption was not tested for leaves containing widely variable pigment content and composition, which makes the limits of reflectance spectroscopy, as well as whether the requirements for spectral regions could be used for estimating contents of four types of foliar pigments—chlorophylls, Chl; carotenoids, Car; anthocyanins AnC; and flavonoids, Flv—uncertain. Thus, development and implementation of reflectance-based techniques requires answering three pivotal questions. First, is it possible to describe the leaf as a medium with a close, linear ρ^{-1} vs. α relationship throughout the visible and near-infrared (NIR) ranges of spectrum, as required by Kubelka-Munk theory? Second, what are the spectral ranges

where the abovementioned requirement is fulfilled? Third, what would be an objective criterion for discerning the ranges where it is not fulfilled? Answering these questions, requiring a thoughtful study of the ρ^{-1} vs. α relationship in leaves with widely variable pigment (Chl, Car, AnC, and Flv) contents, shall reveal the possibilities and limitations of reflectance-based techniques. It may lay a background for informed selection of spectral bands for devising new and improving existing models for reflectance-based estimation of pigments as well as for developing absorbance-based techniques applicable in cases where reflectance-based approaches fail.

Attempts to apply nondestructive methods based on optical spectroscopy for assessment of plant physiological state via measuring pigment content have been undertaken for several decades [30–34]. The situation has changed drastically during the last few decades, when a significant amount of research was dedicated to the development of techniques for nondestructive evaluation of leaf pigments. Here, we provide an overview of foliar absorbance and reflectance spectral features with an emphasis on *in situ* specific optical properties of the pigments. We also give the rationale for quantitative responses of absorbance and reflectance to each pigment content. Based on this, we demonstrate possibilities and limitations of reflectance- and absorbance-based approaches for estimating foliar pigment content. We attempt to find the spectral regions where assumption of a close linear ρ^{-1} vs. α relationship holds so reflectance spectroscopy provides accurate estimation of foliar pigment content. Furthermore, we tackle quantification of the pigments that absorb in spectral regions where reflectance is insensitive to the pigment content. In these regions, absorbance-based techniques are the only way to nondestructively assess pigment content. In view of these limitations, we present models for accurately estimating Chl, Car, AnC, and Flv, as well as generic algorithms for estimating Chl and AnC. Finally, we compare the efficiency of informative spectral band selection for pigment estimation by established methods (neural networks, partial least-square [PLS] regression, vegetation indices, uninformative variable elimination PLS) with that of the specific spectral responses introduced in this chapter.

5.2 SPECTRAL CHARACTERISTICS OF LEAVES

Three data sets were used in this study: Virginia creeper [*Parthenocissus quinquefolia* (L.) Planch.] with a widely varying content of pigments, especially of AnC and Flv [35]*; ANGERS recorded in 2003 at INRA in Angers (France), including 308 leaves of more than 40 plant species [36], as well as transmittance and reflectance spectra†; and the data set composed of 90 leaves (beech, chestnut, and maple) described in [29,37].‡

The leaves of the Virginia creeper illustrate how variable the inherent (absorbance and transmittance) and apparent (reflectance) optical properties are (Figure 5.1). In the blue range (400–500 nm), absorbance was very high, varying widely between 1 and 3 and increasing toward shorter wavelengths in all leaves studied. It was affected by Chl, Car, and Flv. Accordingly, transmittance of the leaves was below 0.1 and varied about 10-fold. In contrast, reflectance of the leaves converged to a narrow range around 0.1, showing small variability.

In the green range (500–600 nm), the absorbance and transmittance varied widely, with two ranges of convergence—around 500 and 600 nm, where the change in pigment content only slightly affected both traits (Figure 5.1a and b). Optical properties around 500 nm were governed by Chl, Car, and AnC and beyond 530 nm—by Chl and especially AnC, whose absorption *in situ* peaks around 550 nm [40]. Reflectance in the green was variable, but much less than absorbance and transmittance.

In the red range (600–690 nm), optical properties were affected by Chl absorption that peaked *in situ* around 670 nm (e.g., [38,39]); the magnitude of the absorbance peak increased gradually

* https://www.researchgate.net/publication/319213426_Foliar_reflectance_and_biochemistry_5_data_sets
† ANGERS Leaf Optical Properties Database (ecosis.org)
‡ https://www.researchgate.net/publication/319619724_Dataset_of_foliar_reflectance_spectra_and_corresponding_pigment_contents_for_Aesculus_hippocastanum_Fagus_Silvatica_Acer_platanoides_published_widely

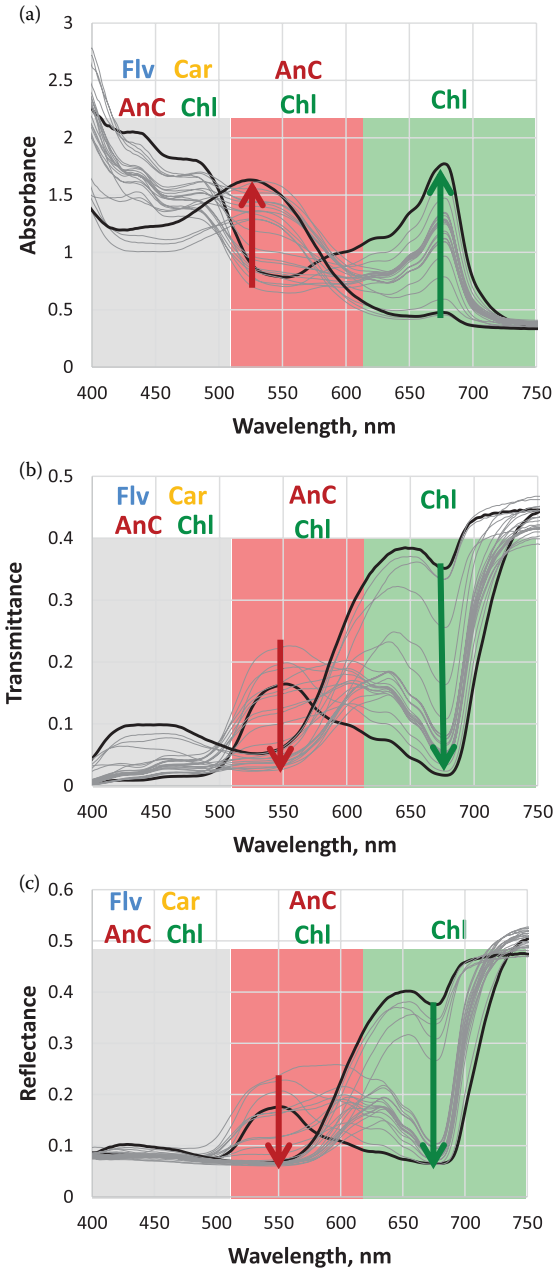

FIGURE 5.1 (a) Absorbance, (b) transmittance, and (c) reflectance spectra of 24 Virginia creeper leaves with widely varying pigment contents and composition. The spectral range shaded with green is solely governed by chlorophylls, Chl; the range shaded with red is governed predominantly by anthocyanins, AnC (when they are present) and Chl; the range shaded in gray is governed jointly by Chl, Car, and flavonoids, Flv, as well as AnC in the long-wave part of blue region. Arrows show direction of increasing leaf pigment content.

with the increase in [Chl] (Figure 5.1a). In the transmittance spectra, Chl absorption manifested itself as a trough whose depth steadily grew with an increase in [Chl] and transformed into a deep minimum in the spectra of leaves with a high [Chl] (Figure 5.1b). In the reflectance spectra, Chl absorption revealed itself as a trough (in the case of low-to-moderate [Chl]), although in the case of leaves with moderate-to-high [Chl], reflectance in the red converged to a narrow range

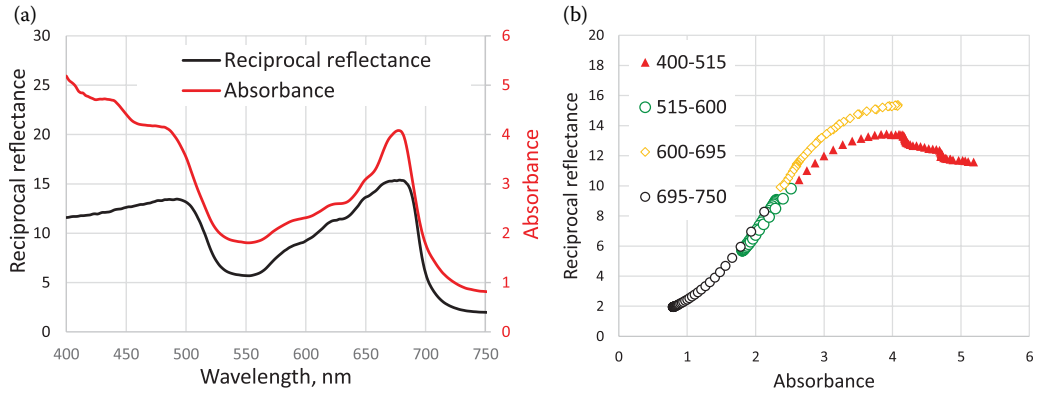

FIGURE 5.2 (a) Absorbance and reciprocal reflectance spectra of Virginia creeper leaf with a moderate [Chl] = 22 μg cm^{-2} and [Car] = 5 μg cm^{-2}, a very high [Flv] = 165 μg cm^{-2}, and a small [AnC] = 0.07 μg cm^{-2}; (b) reciprocal reflectance vs. absorbance of the same Virginia creeper leaf.

around 0.1 (Figure 5.1c). Thus, the behavior of reflectance in the red range differed from that of absorbance or transmittance.

The differences in the spectra depicting absorbance and reflectance were further studied in leaves with contrasting pigment content and composition (Figures 5.2 and 5.3). We compared absorbance and reciprocal reflectance of representative leaves from these data sets. In the Virginia creeper leaf with a moderate [Chl], α and ρ^{-1} were closely related in a linear manner in spectral ranges between 690–750 nm and 515–600 nm (determination coefficient $R^2 = 0.98$)—Figure 5.2. However, at wavelengths shorter than 515 nm and between 600 and 695 nm, the slope of the α vs. ρ^{-1} relationship decreased (Figure 5.2b). A strong hysteresis appeared in the range 600–695 nm: for the same absorbance, reciprocal reflectance was significantly higher than in the blue range 400–515 nm. Moreover, in the shortwave blue range with $\alpha > 2$, ρ^{-1} decreased with an increase in absorbance (Figure 5.2). Thus, in Virginia creeper leaves with $\alpha \geq 1$, reciprocal reflectance cannot be considered as a proxy for absorbance.

The ANGERS data set contained leaves with a wide [Chl] and [Car] variation ([31], Figure 5.3). In the spectral ranges 520–560 nm and 695–750 nm, the ρ^{-1} vs. α relationship was linear, with $R^2 = 0.99$ (Figure 5.3b). In the range 560–695 nm, the relationship was essentially nonlinear

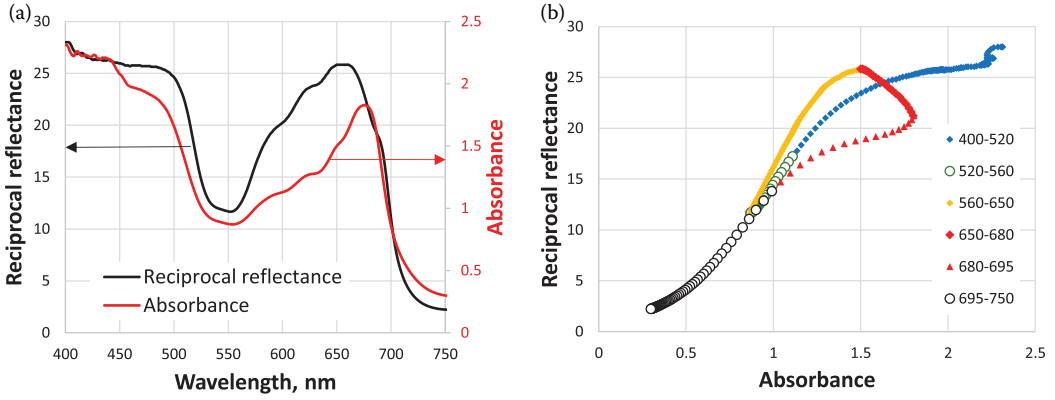

FIGURE 5.3 (a) Absorbance and reciprocal reflectance spectra of a leaf from the ANGERS data set with a high [Chl] = 54 μg cm^{-2} and [Car] = 12 μg cm^{-2}, and a small [AnC] = 2.2 μg cm^{-2}; (b) reciprocal reflectance vs. absorbance of the same leaf.

with a strong hysteresis and negative slope between 650–680 nm. At shorter wavelengths (beyond 520 nm), the slope of the relationship decreased drastically and was close to zero at wavelengths $\lambda < 500$ nm; that is, ρ^{-1} remained virtually invariant while absorbance varied widely (Figure 5.3a).

Thus, in both leaves of nonrelated species (Figures 5.2 and 5.3), the ρ^{-1} vs. α relationships were *close and linear in the green* (520–560 nm) *and red edge* (695–750 nm) ranges and *essentially nonlinear in the blue and red*. This circumstance imposes a very strict limitation on the possibility of foliar pigment content retrieval via reflectance spectroscopy.

5.3 *IN SITU*-SPECIFIC OPTICAL PROPERTIES OF FOLIAR PIGMENTS

ANGERS is a data set with probably the widest [Chl] variation among existing data [36]. However, it does not represent leaves with moderate-to-high [AnC]: only in 12 of 308 leaves [AnC] exceeded 5 $\mu g\ cm^{-2}$, with a maximal value of 17 $\mu g\ cm^{-2}$. Thus, we used this data set to study optical properties of leaves with high variability of [Chl] and [Car] contents against a slightly variable background of [AnC]. The Virginia creeper leaves had widely variable AnC content [35]; in addition, it is the only data set we know where [Flv] and optical properties are presented. This data set was used to study *in situ* optical properties of Flv and AnC.

To quantify the effect of each pigment's content, [p], on absorbance and reciprocal reflectance, α vs. [p] and ρ^{-1} vs. [p] relationships were established at each wavelength (λ) and for each pigment. We calculated the determination coefficient (R^2) for linear relationships α vs. [p] and ρ^{-1} vs. [p] and the slopes of these relationships at each λ. R^2 is a quantitative measure of how well the best-fit function performs as a predictor of α or ρ^{-1}, specifically, how much of their variability can be explained by the variation in the corresponding pigment content. Slopes of α vs. [p] and ρ^{-1} vs. [p] relationships represent sensitivity of absorbance and reciprocal reflectance to the pigment content. However, none of the parameters, either R^2 or the slope, is an accurate quantitative measure of each pigment's effect on α and ρ^{-1}. The spectra of the slope per se do not impart the strength of the corresponding relationships, as the R^2 spectra bear no information about the sensitivity of α or ρ^{-1} to each pigment's content. The quantitative measure of the effect of each pigment on absorbance combining these two parameters is a slope/NRMSE ratio for the α vs. [p] relationship [35], which can be calculated at each wavelength:

$$R\alpha = (d\alpha/d[p])/NRMSE \tag{5.1}$$

where $R\alpha$ is the response of α to a pigment content [*p*], and $d\alpha/d[p]$ and NRMSE are the first derivative and normalized root mean-square error of the α vs. [p] relationship, respectively.

In the same way, the quantitative measure of the effect of each pigment on reciprocal reflectance is the slope/NRMSE ratio of the ρ^{-1} vs. [p] relationship at the corresponding wavelength:

$$R\rho^{-1} = (d\rho^{-1}/d[p])/NRMSE \tag{5.2}$$

where $R\rho^{-1}$ is the response of ρ^{-1} to a pigment content [*p*], and $d\rho^{-1}/d[p]$ and NRMSE are the first derivative and normalized root mean-square error of the ρ^{-1} vs. [p] relationship.

Both measures, $R\alpha$ and $R\rho^{-1}$, represent the spectral response of absorbance and reciprocal reflectance to the content of a specific pigment.

The first question that needed an answer was how α and ρ^{-1} responded to [Chl] and how close the α vs. [Chl] and ρ^{-1} vs. [Chl] relationships are. We carried it out for the ANGERS data set [31] with the widest [Chl] variation. The spectra of R^2, α response ($R\alpha$), and ρ^{-1} response ($R\rho^{-1}$) to [Chl] are presented in Figure 5.4. The main feature of both traits was the disparate spectral behavior of $R\alpha$ and $R\rho^{-1}$. In the blue range (400–500 nm), R^2 for the α vs. [Chl] relationship was above 0.7, but

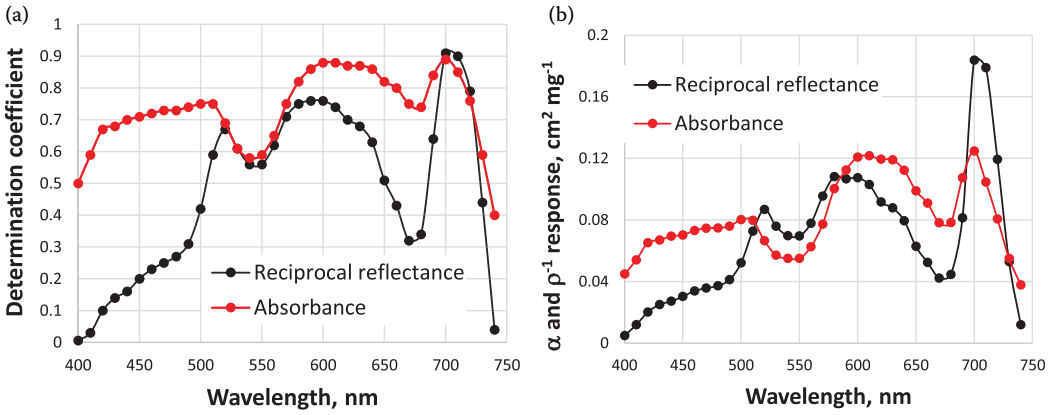

FIGURE 5.4 Characteristics of α vs. [Chl] and ρ^{-1} vs. [Chl] relationships calculated for 308 leaves constituting the ANGERS data set: (a) spectra of determination coefficient, and (b) spectra of α response, Rα, and ρ^{-1} response, $R\rho^{-1}$, to Chl content.

it was below 0.3 for the ρ^{-1} vs. [Chl] relationship (Figure 5.4a). The same was the case in the range 600–680 nm. Only *in the green and red edge ranges* the R^2 of both the α vs. [Chl] and ρ^{-1} vs. [Chl] relationships comparable, reaching R^2 around 0.9 in the red edge range, 700–710 nm. Importantly, (i) in the ranges of highest Chl absorption—the blue (400–500 nm) and the red (around 670 nm)—Rα response to [Chl] was twofold higher than $R\rho^{-1}$ response (Figure 5.4b), and (ii) the green edge and red edge (700–710 nm) were the only spectral ranges where $R\rho^{-1} > R\alpha$ and Chl was the main factor governing ρ^{-1} (Figure 5.4b).

The next step was to compare the spectral response of reciprocal reflectance to the contents of all three pigments identified in the ANGERS data set (Figure 5.5). The $R\rho^{-1}$ spectra for Chl, $R\rho^{-1}$(Chl), and Car, $R\rho^{-1}$(Car) were almost identical. It is not surprising because in the Angers data set, [Car] correlated very closely ($R^2 > 0.9$) with [Chl]. Thus, [Chl] and [Car] were not really independent variables in this data set. Chl and Car contents often vary synchronously during ontogeny and senescence [7,9]. Such a conservative pigment composition is expected since the photosynthetic pigment apparatus is under tight regulation to achieve both maximum efficiency of carbon fixation by and mitigate the risk of photooxidative damage to the leaf [7].

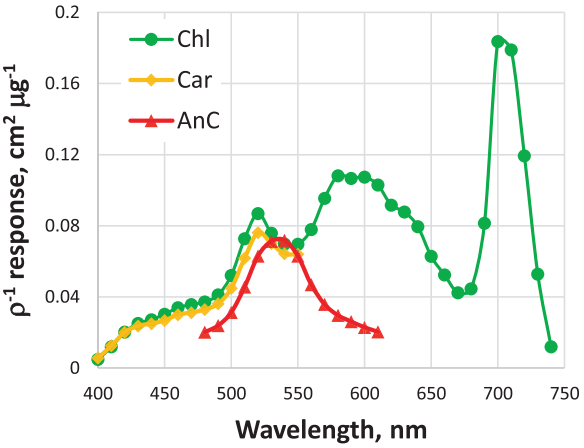

FIGURE 5.5 Spectral response of reciprocal reflectance, $R\rho^{-1}$, to Chl, Car, and AnC contents calculated for 308 leaves constituting the ANGERS data set.

The main spectral feature of the $R\rho^{-1}$ spectra was low values of this trait in the blue (absorption bands of Chl and Car) and red (absorption band of Chl) ranges (Figure 5.5). Two distinguishable peaks of $R\rho^{-1}$(Chl) were around 600 and 700 nm. Importantly, both peaks were positioned in the ranges where absorption by Chl is much smaller than in the red absorption band of this pigment, where leaf reflectance is saturated at small [Chl] $< 20\ \mu g\ cm^{-2}$ [39].

$R\rho^{-1}$(AnC) was high in the green range, around 550 nm (the main AnC absorption region *in situ*) [40,41]. However, $R\rho^{-1}(AnC) \cong R\alpha(Chl)$, so ρ^{-1} in this region was affected by Chl to the same degree as by AnC.

The responses $R\alpha$ and $R\rho^{-1}$ to [Chl], [AnC], and [Flv] were compared for Virginia creeper leaves with highly variable [AnC] and [Flv] and low-to-moderate [Chl]. As for the Angers data set containing leaves with much higher [Chl], $R\alpha$(Chl) was higher than $R\rho^{-1}$(Chl) in the ranges of highest Chl absorption, blue and red (Figure 5.6a). $R\rho^{-1}(Chl) > R\alpha(Chl)$ around 640 and 700 nm, located far from the red Chl absorption band. Notably, both α and ρ^{-1} responses to Chl were negative in the green range (Figure 5.6b) due to the negative slopes of α vs. [Chl] and ρ^{-1} vs. [Chl] relationships (with increases in [Chl], both responses, α and ρ^{-1}, decreased). A majority of leaves in this data set had high amounts of [AnC] and small amounts of [Chl], and leaves with moderate [Chl] contained small AnC. In leaves with small [Chl], absorbance in the green range was high, governed by [AnC], and with increasing [Chl], it decreased due to decreasing [AnC].

$R\alpha(AnC) > R\rho^{-1}(AnC)$ was recorded in the range 520–560 nm, where absorption of AnC peaks *in situ* (Figure 5.6b) due to saturation of reflectance at high [AnC] when α exceeded 2.5. In the range 400–460 nm, $R\alpha$(Flv) was five- to sevenfold higher than $R\rho^{-1}$(Flv) (Figure 5.6c). In this range Chl, Car, and Flv absorbance and reflectance saturated at a low [Chl] even in slightly green leaves; thus, ρ^{-1} became almost invariant with respect to pigment content (Figure 5.1c). This is illustrated well in Figure 5.7b, where $R\rho^{-1}$(Chl) and $R\rho^{-1}$(Flv) were indistinguishable and very small. In contrast, the responses of absorbance $R\alpha$(Chl) and $R\alpha$(Flv) were much higher, and in the narrow spectral range 400–430 nm, response $R\alpha$(Flv) was higher than that of $R\alpha$(Chl) (Figure 5.7a). This finding gives an important insight into identification of a spectral range suitable to [Flv] retrieval from absorbance spectra.

Above, we compared absorbance and reflectance vs. pigment content relationships in leaves using large data sets collected across plant species, developmental stages, and physiological states. The analysis made obvious certain limitations of reflectance-based quantification of the foliar pigments, especially in the blue and red manifesting itself as a failure of the close linear relationship between reciprocal reflectance and absorbance. These limitations can be understood in the frame of Kubelka-Munk theory, which was developed for the case of a relatively weak absorber evenly distributed in a thick layer of a highly reflective substance [27]. Considering the large extinction coefficients of Chl and other pigments [42], their high content in and structural complexity of the leaf and its photosynthetic apparatus [43], it becomes clear that in many cases, the foliar pigments violate these assumptions. Indeed, leaves with absorbance exceeding unity are rather "strong absorbers" in Kubelka-Munk terminology, and distribution of pigments in the cells is far from uniform [13,38]. Furthermore, superficial structures of plants such as leaf cuticle give rise to backscattering [44]. The contribution of light backscattered by weakly pigmented superficial structures of the leaf (cuticle and epidermis) to the total leaf reflectance bears no information about the leaf pigment composition and decreases the "information payload" of total reflected signal. This contribution increases dramatically toward shorter wavelengths of the visible part of the spectrum but bears scarce information on the biochemical composition of the leaf.

These limitations obviously affect the spectral ranges suitable for [Chl], [Car], [AnC], and [Flv] estimation. As a result, a reflectance-based approach can be implemented only in certain spectral ranges positioned outside the main absorption bands of the pigments, mainly in the long-wave part of the visible range, red edge, and NIR [33,34]. In view of these restrictions, it is important to have a quantitative criterion of the suitability of a certain spectral range for application of the reflectance-based techniques, which has not been defined so far. In this work, we try to close this gap by suggesting traits $R\alpha$ and $R\rho^{-1}$ as quantitative measures of the α and ρ^{-1} response to content of each pigment.

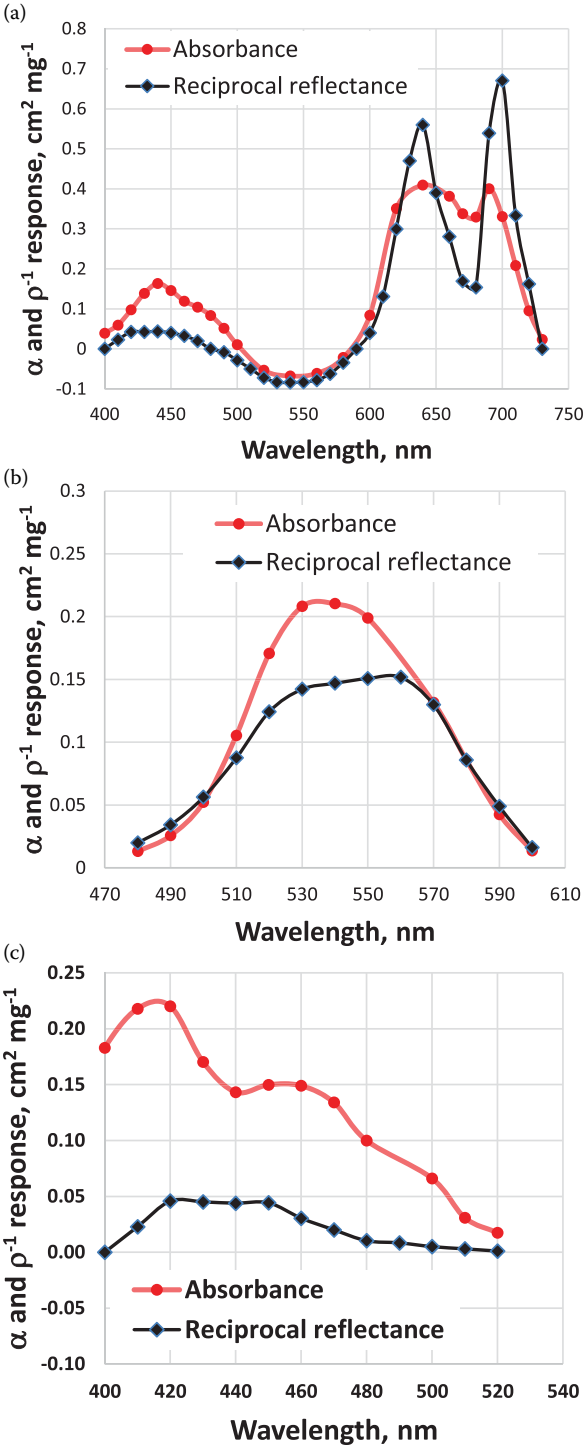

FIGURE 5.6 Spectra of absorbance response, $R\alpha$, and reciprocal reflectance response, $R\rho^{-1}$, to content of (a) chlorophyll [Chl], (b) anthocyanin [AnC], and (c) flavonoids [Flv] in 24 leaves of Virginia creeper with highly variable [AnC] and [Flv] and low to moderate [Chl].

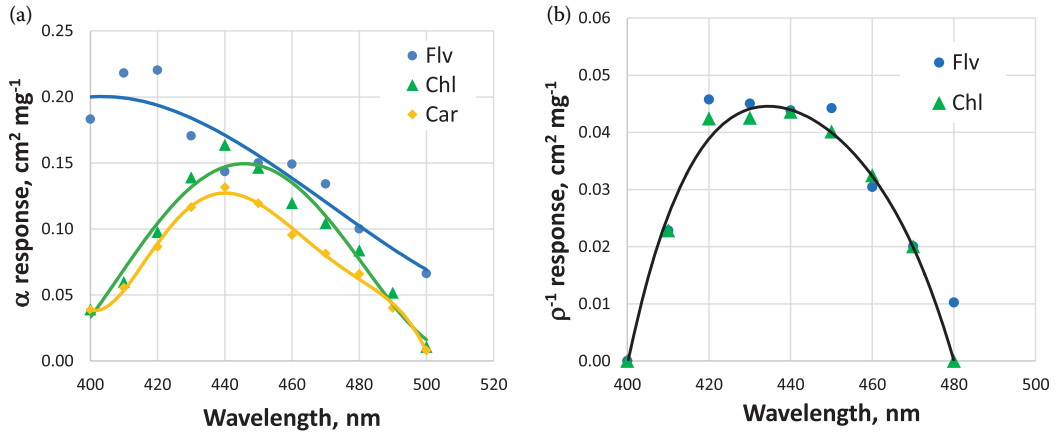

FIGURE 5.7 The responses of absorbance, Rα (a), and reciprocal reflectance, $R\rho^{-1}$ (b), to pigment contents in the blue range of the spectrum in 24 Virginia creeper leaves. Note that ρ^{-1} responses to Flv and Chl are identical, showing that there is no way to distinguish between these pigments using reflectance, whereas the Rα response to Flv in the range 400–430 was higher than that to Chl. ((a): Modified from A. Gitelson et al. *Journal of Plant Physiology*, 218: 2017, 258–264. [35])

It was shown that responses Rα and $R\rho^{-1}$ to Chl are very different across the spectral region and greatly depend on pigment content and composition. Thus, spectral responses Rα and $R\rho^{-1}$ complement specific absorption coefficients, bringing the quantitative effect of each pigment *with background of other pigments* on α and ρ^{-1}. These findings using quantitative spectral responses to each pigment group are in accord with the results of previous studies that identified optimal spectral bands for retrieval of foliar pigment content [19,34,45,46].

5.4 PIGMENT CONTENT ESTIMATION

5.4.1 CHLOROPHYLLS

For individual leaves and two contrasting data sets, it was shown that responses Rα(Chl) and $R\rho^{-1}$(Chl) are very different across the whole spectral range and greatly depend on pigment content and composition. Essentially, in the *red edge region* (around 700 nm), $R\rho^{-1} > R\alpha$ (Figures 5.4b and 5.6a) and the spectral shape and magnitude of the responses were almost identical despite great variation in pigment content in the data sets studied. This means that ρ^{-1} in the red edge region may be used as a term in algorithms for accurate and, probably, generic measure of [Chl] (Figures 5.8a and 5.9a). The only obstacle to achievement of a high accuracy of [Chl] estimation using ρ^{-1} is nonzero values of absorbance and reciprocal reflectance in the near-infrared spectral range where Chl does not absorb (Figure 5.1a). Merzlyak, Chivkunova, Melo, and Naqvi [47] have shown that this is apparent absorbance caused by uncertainties of absorbance and reflectance measurement. These uncertainties may affect accuracy of [Chl] estimation, especially for low-to-moderate [Chl] [29]. Thus, for accurate [Chl] estimation subtraction of α_{NIR} and ${\rho_{NIR}}^{-1}$ (NIR beyond 760 nm) from α_{RE} and ${\rho_{RE}}^{-1}$ (RE around 710 nm), is required:

$$\text{Chl} \propto \alpha_{RE} - \alpha_{NIR} \tag{5.3}$$

$$\text{Chl} \propto {\rho_{RE}}^{-1} - {\rho_{NIR}}^{-1} \tag{5.4}$$

Subtraction of α_{NIR} and ${\rho_{NIR}}^{-1}$ makes $(\alpha_{RE} - \alpha_{NIR})$ and $({\rho_{RE}}^{-1} - {\rho_{NIR}}^{-1})$ almost proportional to [Chl] (i.e., the relationships go to the origin) and it brings a significant increase in accuracy (Figures 5.8b

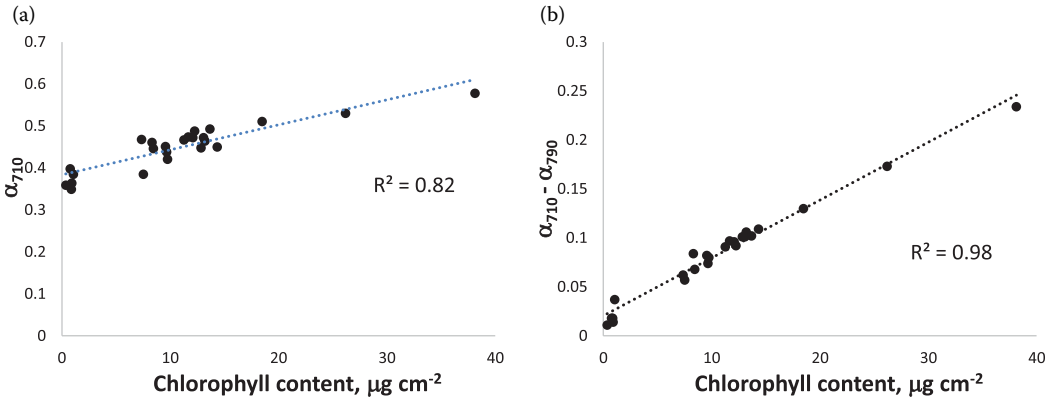

FIGURE 5.8 Chlorophyll content in the Virginia creeper leaves plotted versus (a) absorbance at 710 nm, α_{710}; (b) difference of absorbance at 710 nm and in the NIR at 790 nm, $\alpha_{710}-\alpha_{790}$.

and 5.9b). Both models yield very accurate [Chl] estimation using absorbance and reflectance, with the determination coefficient above 0.98 and NRMSE $< 2.4\%$.

A three-band model was suggested for estimating [Chl] in the form [29]:

$$\text{Chl} \propto (\rho_{RE}^{-1} - \rho_{NIR}^{-1}) \times \rho_{NIR} \tag{5.5}$$

The third item, ρ_{NIR}, was introduced to take into account variability in leaf thickness and density that could affect [Chl] estimation. In leaves with the same [Chl] and different thickness/density, [Chl] retrieved from Equation 5.4 is smaller in thicker leaf than that in a thinner leaf. NIR reflectance of thicker leaves is higher than in thinner leaves, and the use of ρ_{NIR} allows decreasing uncertainty caused by variation in leaf thickness (Figures 5.9c and 5.10c). Reciprocal reflectance ρ_{710}^{-1} alone was also a very accurate measure of [Chl] in the ANGERS data set with a wide [Chl] variability (Figure 5.10a). To increase accuracy, we applied Equation 5.4 with a red edge band at 710 nm and NIR at 770–800 nm, estimating [Chl] in this data set (Figure 5.10b). The accuracy was very high ($R^2 = 0.94$), confirming the robustness of the approach. $CI_{\text{red edge}}$ taking into account different leaf thickness/density was the most accurate (Figure 5.10c).

Different techniques for foliar [Chl] estimation, neural network (NN), partial least-squares regression, and vegetation indices (VIs), for three unrelated plant species (maple, chestnut, and beech) were tested in [32]. Descriptive statistics of the relationships between pigment content estimated by all three techniques are presented in Table 5.1. All three techniques were found to estimate [Chl] accurately (Figure 5.11). Among the VIs tested, $CI_{\text{red edge}}$ was the most accurate. Compared to NN and PLS, $CI_{\text{red edge}}$ was also superior, with almost zero bias and a coefficient of variation (CV) below 12.1%. NN and PLS were very accurate, with CV below 11.8% for NN, with 8.9% positive mean normalized bias (MNB), and CV below 12.5% for PLS, with 9% negative MNB.

5.4.2 Carotenoids

Among other pigments, carotenoid estimation is probably the most challenging due to a strong overlap of Car absorption with those of Chl, AnC, and Flv, as well as the vast chemical (and hence spectral) diversity of Car, which is also easily changed by environmental stimuli. Another obstacle is the quite close relationship between [Chl] and [Car], so these variables are far from independent [48]. Thus, the precise estimation of [Car] with nondestructive spectral measurements has so far not reached accuracies comparable to the results obtained for [Chl] estimation.

It was found that maximal sensitivity of reflectance to [Car] is in the so-called green edge around 510–515 nm (Gitelson et al., 2002). However, reflectance in this range is greatly affected by Chl

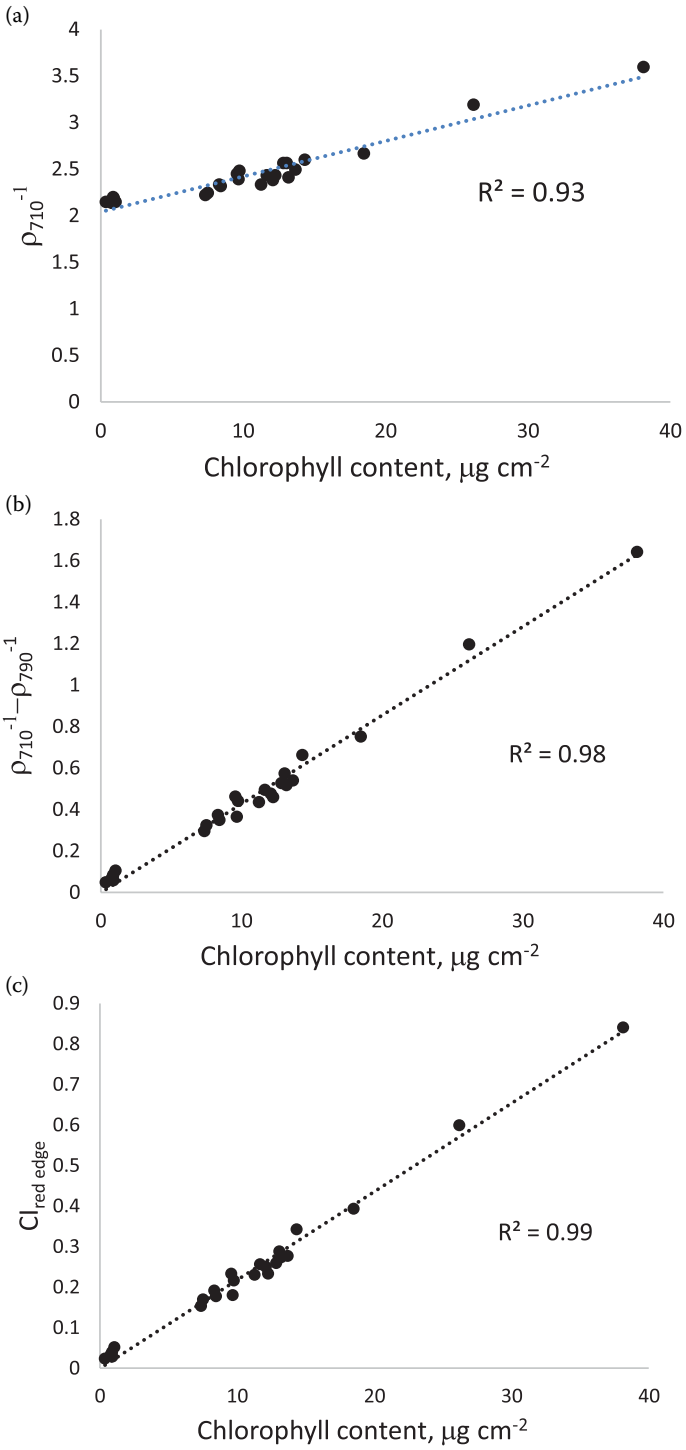

FIGURE 5.9 Chlorophyll content in the Virginia creeper leaves plotted versus (a) reciprocal reflectance at 710 nm, ρ_{710}^{-1}; (b) difference of reciprocal reflectances at 710 nm and in the NIR at 790 nm, $\rho_{710}^{-1} - \rho_{790}^{-1}$; (c) red edge chlorophyll index $CI_{red\ edge} = (\rho_{790}/\rho_{710})^{-1}$.

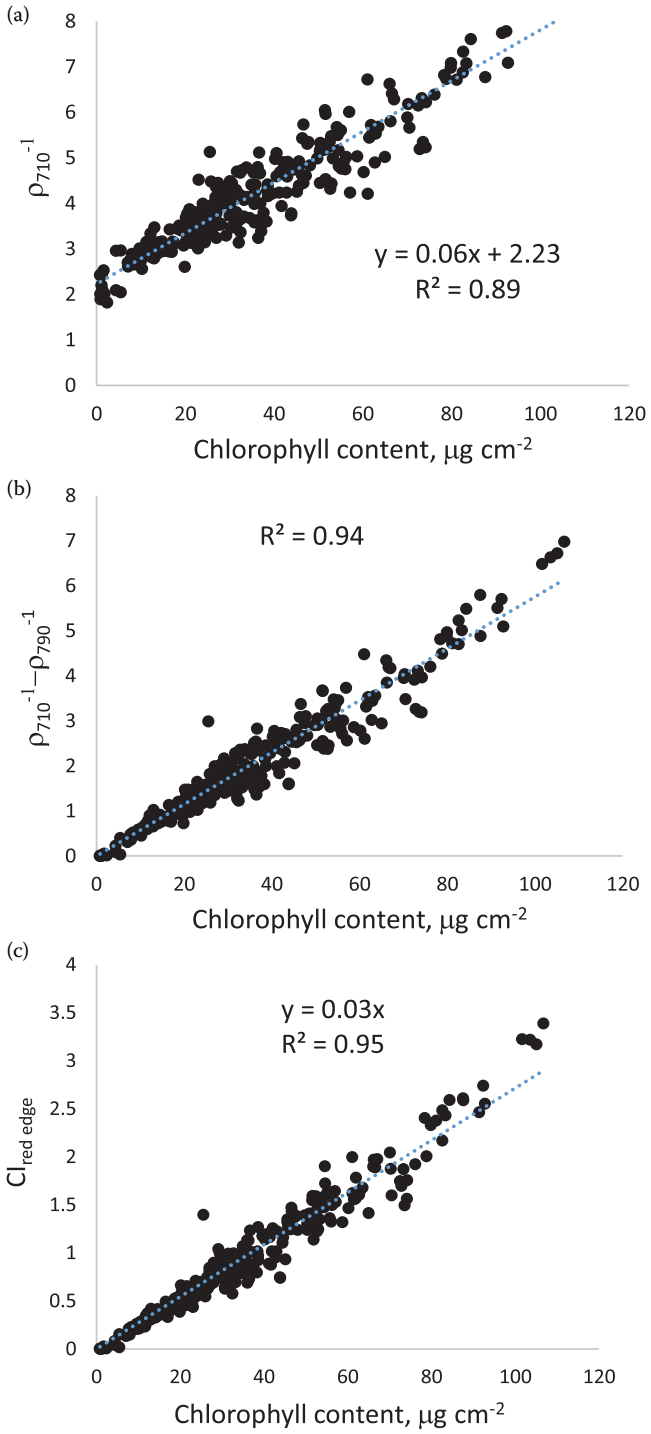

FIGURE 5.10 Chl content in the leaves of the ANGERS data set plotted versus (a) reciprocal reflectance at 710 nm, (b) ρ_{710}^{-1}, difference $\rho_{710}^{-1}-\rho_{790}^{-1}$, and (c) red edge chlorophyll index $CI_{red\ edge} = (\rho_{790}/\rho_{710})-1$.((c): Adopted from A. Gitelson, A. Solovchenko, *Geophysical Research Letters*, 2017. [66])

TABLE 5.1
Descriptive Statistics of the Relationships between Leaf Chlorophyll Content Measured and Estimated by Three Models, NN, PLS, and $CI_{red\ edge}$

	CV	R^2	MNB	NMB
$CI_{red\ edge}$	12.1	0.97	−0.8	−0.1
NN	11.8	0.97	8.9	−0.3
PLS	12.5	0.97	−6.2	0.6

Source: Modified from O. Kira et al. *International Journal of Applied Earth Observation and Geoinformation*, 38: 2015, 251–260. [37]
Note: CV = coefficient of variation, MNB = mean normalized bias, NMB = normalized mean bias; all three measures are in percent.

absorption. Thus, it was suggested to subtract the Chl effect from ρ_{510}^{-1} using reciprocal reflectance in the green and red edge that are quite accurate measures of [Chl]. Carotenoid reflectance indices were suggested in the forms:

$$CRI_{green} \propto (\rho_{510}^{-1} - \rho_{green}^{-1}) \tag{5.6}$$

$$CRI_{RE} \propto (\rho_{510}^{-1} - \rho_{RE}^{-1}) \tag{5.7}$$

To take into account likely differences in leaf thickness/density, CRI was modified and presented as:

$$mCRI_{green} \propto (\rho_{510}^{-1} - \rho_{green}^{-1}) \times \rho_{NIR} \tag{5.8}$$

$$mCRI_{RE} \propto (\rho_{510}^{-1} - \rho_{RE}^{-1}) \times \rho_{NIR} \tag{5.9}$$

However, [Car] was never estimated in AnC-containing leaves. As can be seen in Figure 5.5, ρ^{-1} response to Car and AnC in the range around 515 nm is almost even; thus. subtraction of this effect is necessary. Subtraction of α_{550} from α_{510} allowed quite accurate estimation of [Car] in AnC-containing Virginia creeper leaves (Figure 5.12a).

Kira, Linker, and Gitelson [37] compared accuracy of estimating [Car] by neural network, partial least-squares regression, and VIs in maple, chestnut, and beech leaves. In Table 5.2, descriptive statistics of the relationships between Car content estimated by all three techniques are presented. Relationships between NN and PLS models, red edge carotenoid reflectance index ($CRI_{red\ edge}$), and Car content were very close for each species. However, while $CRI_{red\ edge}$ vs. Car relationships for maple and chestnut had very similar slopes, the slope of the relationship for beech was much lower than for maple and chestnut; thus, the $CRI_{red\ edge}$ vs. Car relationship for all three species taken together was essentially not linear, with CV = 23%. For all three species taken together, NN vs. Car and PLS vs. Car relationships were much closer (with R^2 above 0.91) than that between $CRI_{red\ edge}$ and Car (Figure 5.13).

Fassnacht, Stenzel, and Gitelson [49] addressed the issue of nonlinearity of CRI and mCRI vs. [Car] relationships (Figure 5.13a). Using the same data set as Kira, Linker, and Gitelson [37] they examined the potential of the angular vegetation index (AVI) [49–51] to estimate total foliar [Car] of maple, chestnut, and beech. Based on an iterative search of all possible band combinations, a best-candidate AVI_{car} was identified. The identified index used reflectances at wavelengths 410, 530, and 550 nm and showed a quite close but essentially not linear relation with Car contents of the

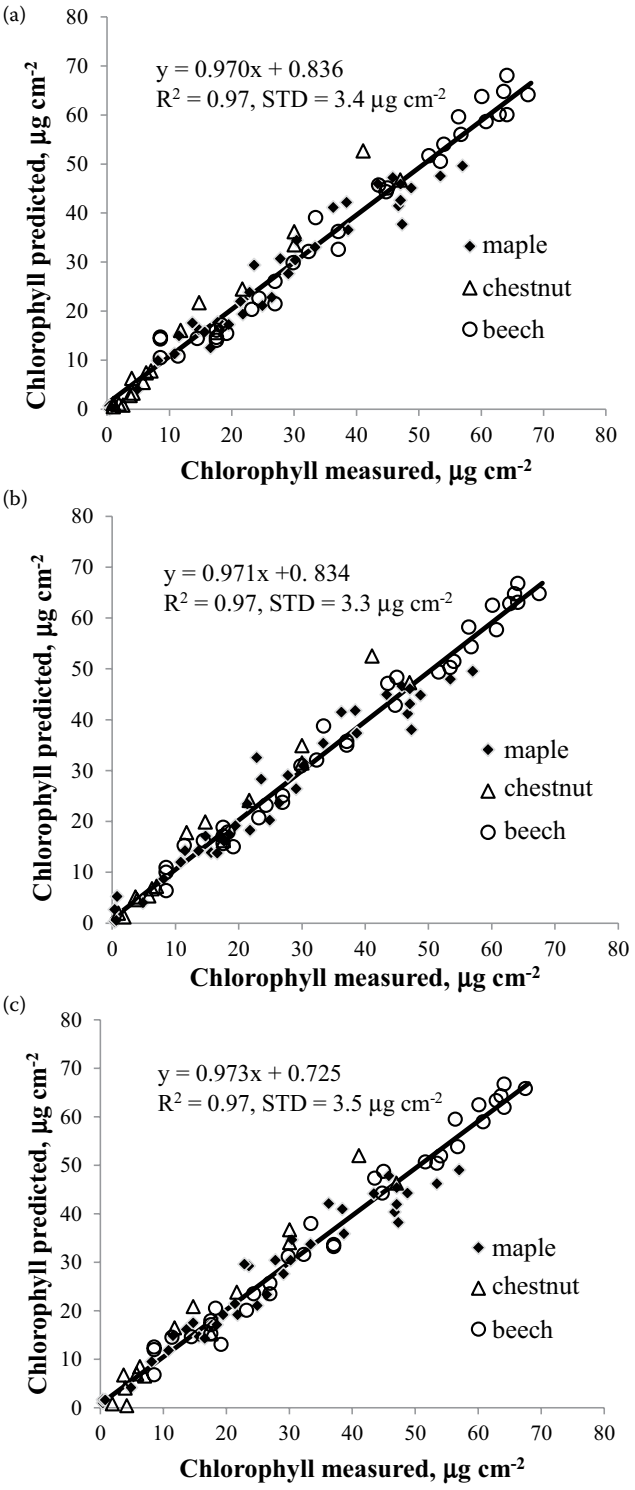

FIGURE 5.11 Chlorophyll content estimated by (a) red edge chlorophyll index, $CI_{red\ edge}$; (b) NN; and (c) PLS plotted versus measured chlorophyll content in maple, chestnut, and beech. (Modified from O. Kira et al. *International Journal of Applied Earth Observation and Geoinformation*, 38: 2015, 251–260. [37])

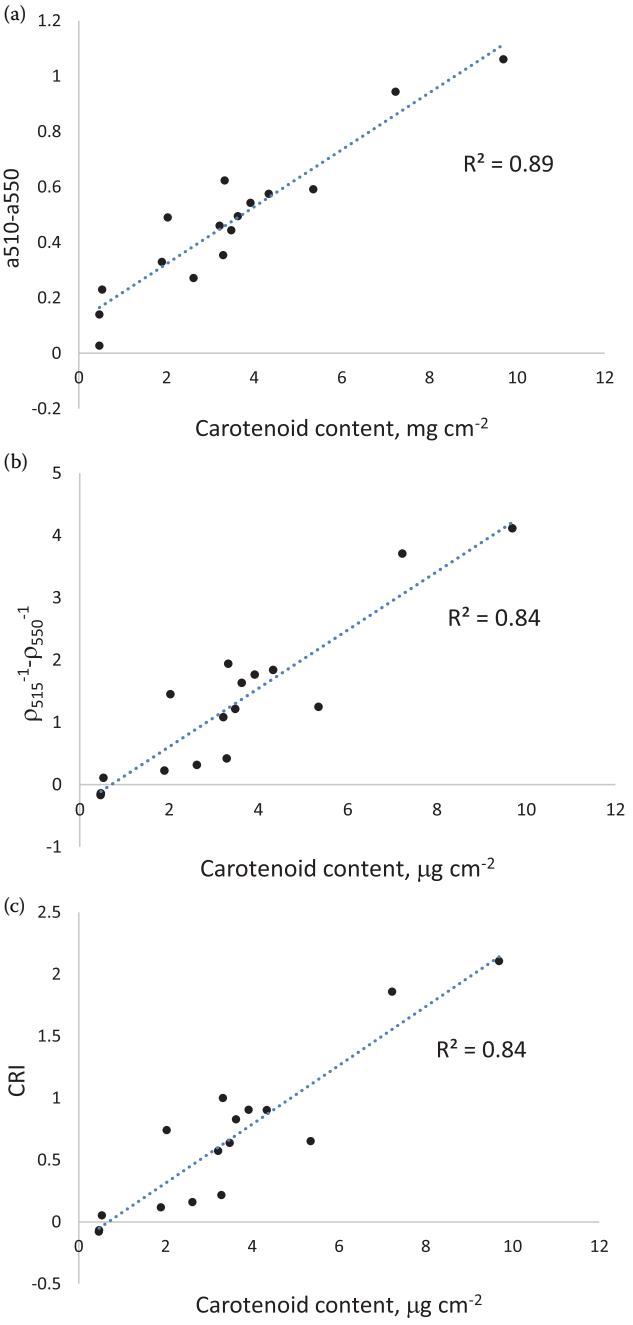

FIGURE 5.12 Carotenoid content in the Virginia creeper leaves plotted versus (a) difference of absorbance $\alpha_{510}-\alpha_{550}$; (b) difference of reciprocal reflectances at 510 and 550 nm, $\rho_{510}^{-1}-\rho_{550}^{-1}$; and (c) green carotenoid reflectance index $CRI_{green} = (\rho_{510}^{-1}-\rho_{550}^{-1}) \times \rho_{770-800}$.

examined species with increasing sensitivity to high [Car] and a lack of sensitivity to low [Car] for which both $mCRI_{RE}$ (Equation 5.9) and ρ_{760}/ρ_{500} [30] performed better. To make use of the advantages of both VI types, a simple merging procedure, which combined AVI_{car} with two earlier proposed carotenoid indices ($mCRI_{RE}$ and ρ_{760}/ρ_{500}), was developed. The merged indices had a close linear relationship with total Car content and outperformed all other examined indices. The merged indices

TABLE 5.2
Descriptive Statistics of the Relationships between Leaf Carotenoid Content Measured and Estimated by Three Models, NN, PLS, and $CRI_{red\ edge}$

	CV	R^2	MNB	NMB
$CRI_{red\ edge}$	24.8	0.70	4.7	0.9
NN	15.6	0.88	1.7	1.4
PLS	16.7	0.86	−4.5	17.7

Source: Modified from O. Kira et al. *International Journal of Applied Earth Observation and Geoinformation*, 38: 2015, 251–260. [37]
Note: CV = coefficient of variation, MNB = mean normalized bias, NMB = normalized mean bias; all three measures are in percent.

were able to accurately estimate total [Car] with a normalized root mean square error (NRMSE) of 8.12% and a coefficient of determination of 0.88 (Figure 5.14). The findings were confirmed by simulations using the radiative transfer model PROSPECT-5. This strengthens the assumption that the proposed merged indices have a general ability to accurately estimate foliar [Car]. To prove the general applicability of the index for nondestructive estimation of Car from leaf reflectance data, further examination of the proposed merged indices for other plant species is desirable.

5.4.3 Anthocyanins

In the Virginia creeper data set containing mainly red and dark red leaves, large differences in $R\alpha(AnC)$ and $R\rho^{-1}(AnC)$ responses in the range 520–550 nm were found (Figure 5.6b). This shows that the highest accuracy of [AnC] estimation may be achieved using absorbance at 550 nm, shown in Figure 5.15a. Reciprocal reflectance around 570 nm, where $R\alpha(AnC) = R\rho^{-1}(AnC)$, was also an accurate proxy of [AnC] (Figure 5.15c). However, Chl significantly affected α and ρ^{-1} in the range 550–570 nm. Thus, subtraction of this effect should be done using α and ρ^{-1} in the red edge range where they accurately represent [Chl]. The following models were capable of accurate estimation of [AnC] using absorbance and reflectance of leaves with widely variable pigment composition (Figure 5.15b and d):

$$[AnC] \propto \alpha_{550} - \alpha_{RE} \tag{5.10}$$

$$[AnC] \propto \rho^{-1}{}_{570} - \rho^{-1}{}_{RE} \tag{5.11}$$

5.4.4 Flavonoids

In the blue range, 400–500 nm, where optical properties are affected by all three pigments, Chl, Car, and Flv, ρ^{-1} was either almost flat (Figure 5.3b) or even decreased with α increase (Figure 5.2b). $R\alpha$ and $R\rho^{-1}$ bring unique quantitative information on the responses of α and ρ^{-1} to [Chl] and [Flv], which is specific for each pigment. As can be seen from Figure 5.7b, the responses $R\rho^{-1}(Chl)$ and $R\rho^{-1}(Flv)$ were equal, showing that reflectance spectroscopy is unable to differentiate between these pigments. By contrast, in the range between 400 and 430 nm, the response $R\alpha(Flv)$ was higher than $R\alpha(Chl)$, suggesting that for the data used, it is the only spectral band where [Flv] may be estimated using absorbance spectroscopy (Figure 5.7a). Another important finding is that Chl's effect in the range 400–430 nm is still significant (Figure 5.7b), and its subtraction would

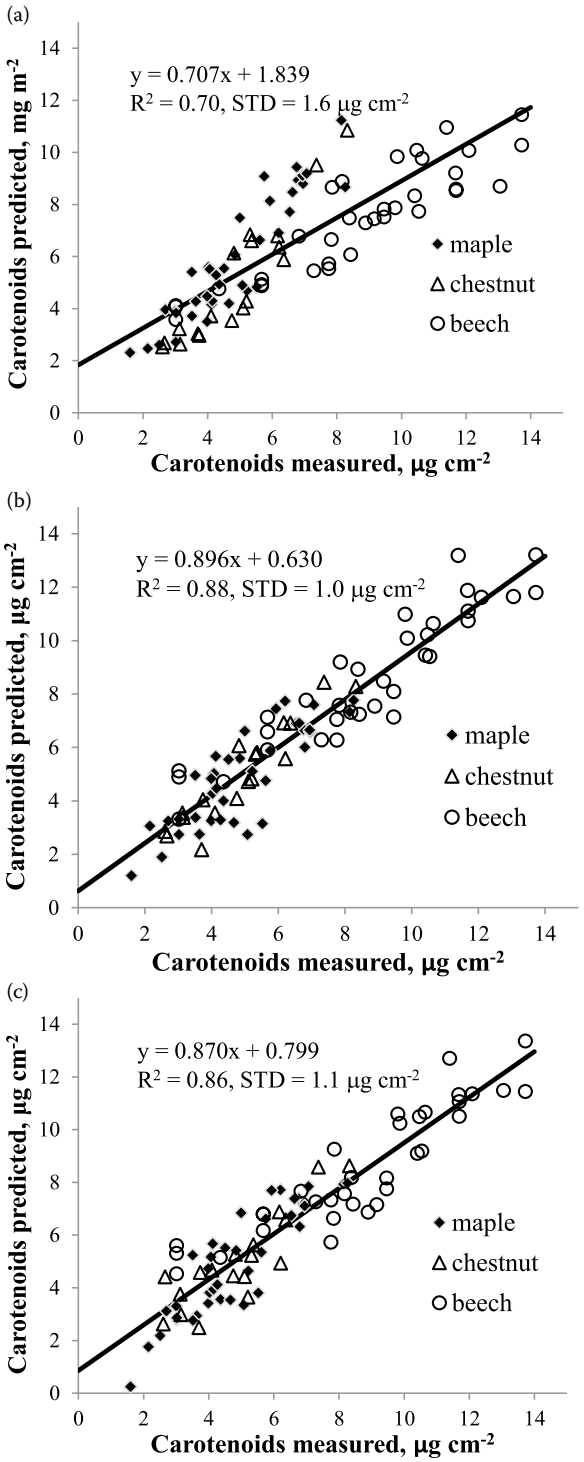

FIGURE 5.13 Carotenoid content estimated by (a) modified green carotenoid reflectance index, CRI_{green}; (b) NN; and (c) PLS plotted versus measured carotenoids content in maple, chestnut, and beech. (Reprinted from O. Kira et al. *International Journal of Applied Earth Observation and Geoinformation*, 38: 2015, 251–260. [37])

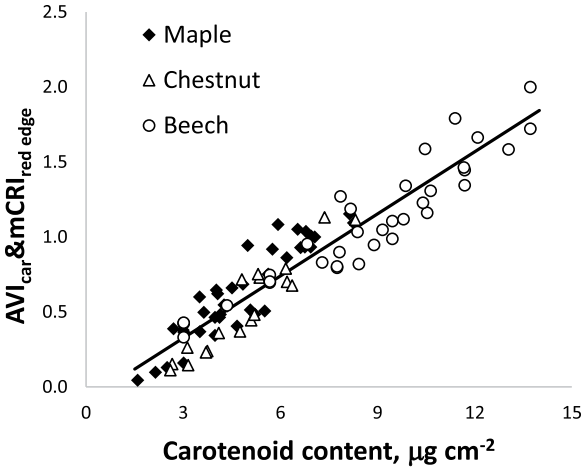

FIGURE 5.14 Merged AVI_{car} and $mCRI_{red\ edge}$ plotted vs. total carotenoid content in maple, chestnut, and beech. The solid line is the linear best-fit function of the relationship between the index and total carotenoid content for all three species taken together. (Modified from F.E. Fassnacht et al. *Journal of Plant Physiology*, 176: 2015, 210–217 [49])

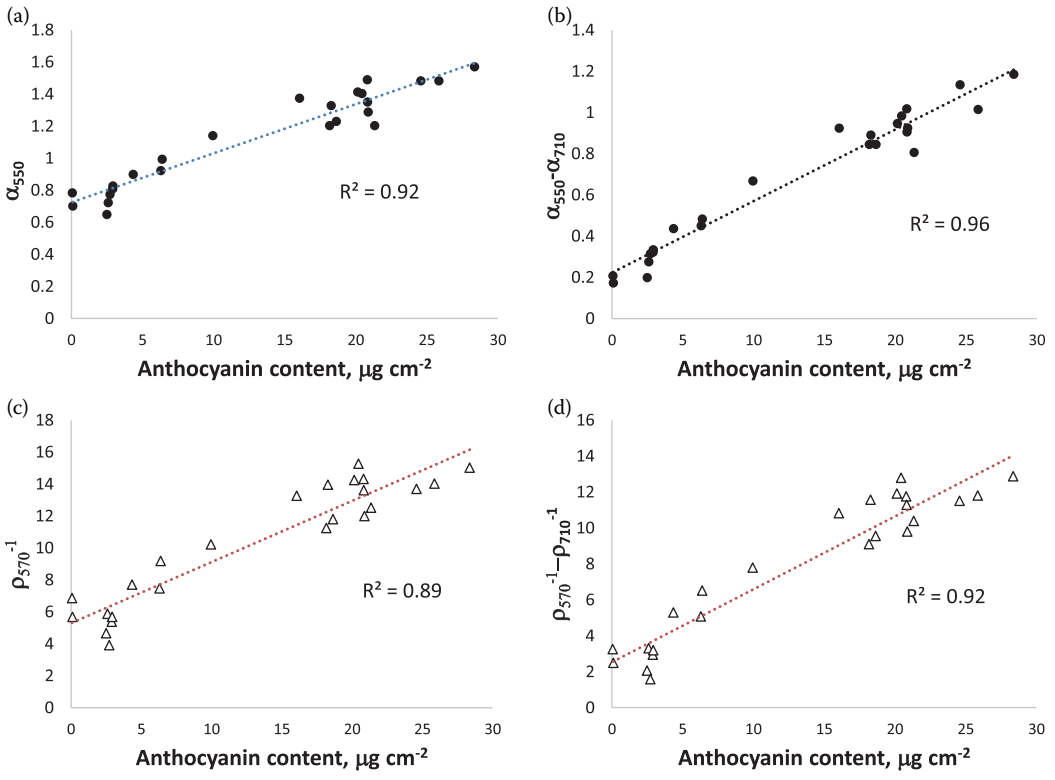

FIGURE 5.15 Anthocyanin content in 24 Virginia creeper leaves plotted versus (a) absorbance at 550 nm, α_{550}; (b) difference of absorbance at 550 and 710 nm, $\alpha_{550}-\alpha_{710}$; (c) reciprocal reflectance at 570 nm, ρ_{570}^{-1}; and (d) difference $\rho_{570}^{-1}-\rho_{710}^{-1}$.

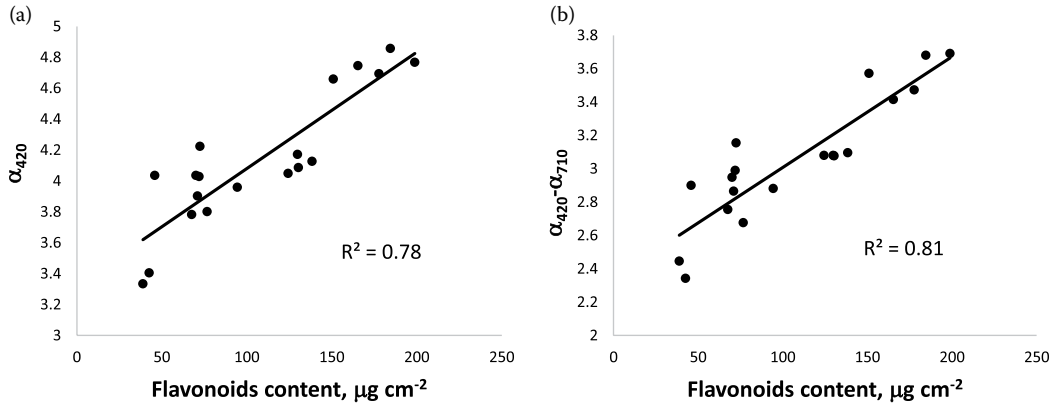

FIGURE 5.16 Flavonoid content in Virginia creeper leaves plotted versus (a) absorbance at 420 nm, α_{420}; (b) difference of absorbance at 420 and 710 nm, $\alpha_{420}-\alpha_{710}$. ((b): Modified from A. Gitelson et al. *Journal of Plant Physiology*, 218: 2017, 258–264. [35])

be necessary for accurate [Flv] estimation. Absorbance at 420 nm was quite an accurate proxy of [Flv] (Figure 5.16a). Subtraction of α_{710} allowed a decreasing Chl effect at 420 nm, and the following model is suggested for accurate nondestructive estimation of [Flv] in a wide range of their variation (Figure 5.16b):

$$[\text{Flv}] \propto \alpha_{420}-\alpha_{710} \tag{5.12}$$

5.5 KNOWLEDGE-BASED SELECTION OF SPECTRAL BANDS

The uninformative variable elimination PLS (UVE PLS) technique is not a band selection per se in the sense that one tries to find the best small subset of variables for fitting a model, but the elimination of those variables that are useless [52]. Kira, Linker, and Gitelson [37] investigated the magnitude of the reliability parameter *as an indicator of the information contained in the spectral bands* and compared the most informative bands with the spectral bands used by the other models (NN, PLS, and VIs—$CI_{\text{red edge}}$ and $CRI_{\text{red edge}}$). The results of UVE PLS for [Chl] and [Car] estimation are presented in Figure 5.17. The green spectral band around 560 nm retained in the NN and PLS models for Chl estimation (red areas in Figure 5.17a) coincided with highest values of the reliability parameter. In this spectral region, reflectance is governed by Chl hyperbolically decreasing with increase of [Chl] [53]. This spectral range was widely used for [Chl] estimation due to the high sensitivity of reflectance to Chl content in a wide range of its change in slightly green to dark green leaves [38,39,54–56].

Another maximum of the reliability parameter was found in the long wave end of the red edge region between 730 and 750 nm, where two factors govern reflectance. They include Chl absorption that is significant in leaves with Chl content above 400 mg m^{-2} (green to dark green leaves), and leaf structure and thickness affecting reflectance in the NIR range [43,55,57]. In previous studies, this band was used for accurately estimating foliar and total canopy Chl and nitrogen content using the red edge Chl index [23,29,58].

Despite the very low magnitude of the reliability parameter in the blue region (Figure 5.17a), the band around 480 nm was retained in the NN and PLS models for [Chl] estimation. In this region, absorption is saturated strongly and sensitivity of reflectance to [Chl] is minimal, as indicated by the magnitude of the reliability parameter. However, the blue range is suitable for reference reflectance in VIs for eliminating partially random variability of reflectance due to uncertainties of measurements as well as differences in leaf surface structure [59].

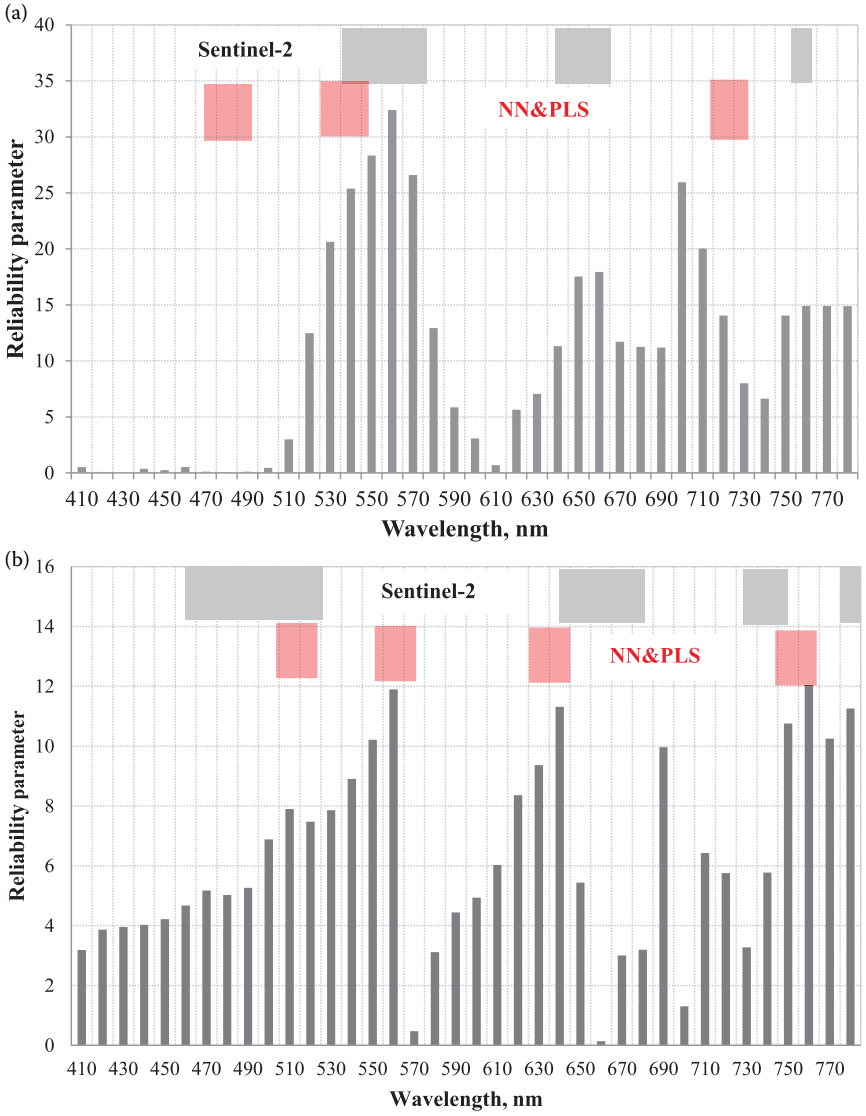

FIGURE 5.17 Reliability parameter calculated using uninformative variable elimination PLS (UVE PLS) plotted versus wavelength for (a) chlorophyll content and (b) carotenoid content estimation. The grey areas at the top correspond to positions of Sentinel-2 bands, which were found optimal for pigment estimation by NN and PLS models (Table 5.3). The red areas indicate the 20-nm-wide spectral bands that were found to be optimal for pigment content estimation by NN and PLS. Data containing maple, chestnut, and beech leaves (e.g., [32,38]) were used.

The reliability parameter for Chl estimation indeed provided a reliable indication of the usefulness of the spectral region: its maxima coincided with the positions of spectral bands used by the green and red edge Chl indices [29,34]. The other bands used in these indices (beyond 770 nm and either 540–560 nm in CI_{green} or 690–730 nm in $CI_{red\ edge}$) also correspond to regions in which the magnitude of the reliability parameter is substantial.

All four spectral bands retained in the NN and PLS models for [Car] estimation coincided with highest values of the reliability parameter (Figure 5.17b), as well as with spectral bands of the red edge CRI and green CRI [60]. The first band retained in the models was located around 510 nm,

where maximal sensitivity of reflectance to [Car] was found [60]. In this region, both Chl and Car contents govern reflectance, and this band was used in both CRI_{green} and $CRI_{red\ edge}$ [34,60].

The second band retained in the models was located in the green range, where the magnitude of the reliability parameter is maximal. This band was used in CRI_{green} for subtraction of Chl's effect from reflectance around 510 nm [33]. The third and fourth spectral bands retained in the NN and PLS models were located around 630 and 740 nm. Both bands are located quite far from the main absorption bands of Chl and Car; at moderate to high Chl content, absorption around 630 and 740 nm is not saturated and thus reflectance in these regions is sensitive to [Chl]. The band centered at 630 nm has an additional advantage—absorption by both Chl *a* and Chl *b* at 630 nm are almost the same. Thus, in contrast to the 740-nm band where only Chl *a* absorbs, the 630-nm band accounts not only for Chl *a* but also for Chl *b* absorption. To the best of our knowledge, the 630-nm band has never been used in any estimation of either Chl or Car contents.

Importantly, the location of the spectral bands retained in the models did not correspond to the main absorption bands of pigments of interest Chl and Car, and this is not surprising. They coincided with the location of spectral bands where absorption by Chl remained strong enough to be sensitive to Chl content but far enough from the main Chl absorption bands to avoid saturation. Remarkably, for Car estimation, the NN and PLS models retained bands centered at 490–510 nm and 470–490 nm, respectively, which are the spectral regions where reflectance was found to be maximally sensitive to Car absorption while also being affected by Chl absorption [30,32,60]. This region is also close to the range where reflectance is sensitive to the xanthophyll cycle and used in the photochemical reflectance index [31].

The repeatability of the wavelength selection for the NN and PLS models is remarkable; they almost completely coincided (Figure 5.17). It is also worth noting that consistent results of Chl and Car estimation by NN and PLS were achieved using reflectance without any spectral transformation, for example, $\log(1/\rho)$, first derivative, second derivative [61]. The band selection was not dependent on the data used, and the bands retained in the NN and PLS models agreed well with those reported in other studies and known to explain the chemical variation in our data sets.

The expected accuracy of pigment content estimation by VIs, NN, and PLS with spectral bands of the multispectral instrument (MSI) on the Sentinel-2 satellite was assessed in [32] and is presented in Table 5.3. $CI_{red\ edge}$ with spectral bands centered at 705 and 775 nm (Table 5.4) was able to estimate

TABLE 5.3

Coefficient of Variation (in Percent) of Chlorophyll and Carotenoid Estimation by Neural Network (NN) and Partial Least-Squares (PLS) Regression with Simulated Expected Spectral Response of the Multispectral Instrument (MSI) aboard the Sentinel-2 Satellite

		CV				CV	
	Bands	**NN**	**PLS**		**Bands**	**NN**	**PLS**
Chlorophyll	B1-B7	13.6	16.0	Carotenoids	B1-B7	19.9	21.0
	B4-B7	13.6	13.6		B4-B7	21.1	21.1
	B5-B7	13.6	13.6		B5-B7	21.0	21.0
	B6-B7	14.1	14.1		B6-B7	20.9	20.9
	B5-B6	26.9	26.8		B5-B6	27.9	28.0
	B4-B6	20.9	20.9		B4-B6	25.9	25.9
	B2, B4, B6-B7	13.7	13.7		B2, B5, B6-B7	20.5	20.4
	B3, B6, B7	13.6	13.6		B2, B4, B6-B7	19.6	19.6
	B3, B5, B7	21.5	21.4				

Source: Reprinted from O. Kira et al. *International Journal of Applied Earth Observation and Geoinformation*, 38: 2015, 251–260. [37]

Note: The spectral bands of MSI are given in Table 5.4.

TABLE 5.4
Specifications of the Seven Spectral Bands (B1–B7) of the Multispectral Instrument (MSI) aboard the Sentinel-2 Satellite

Spectral Band	Center Wavelength (nm)	Band Width (nm)	Spatial Resolution (m)
B1	443	20	60
B2	490	65	10
B3	560	35	10
B4	665	30	10
B5	705	15	20
B6	740	15	20
B7	783	20	20

Source: Reprinted from O. Kira et al. *International Journal of Applied Earth Observation and Geoinformation*, 38: 2015, 251–260. [37]

[Chl] with CV = 13.1%, and using spectral bands at 740 and 775 nm CV was even lower − 12.6%. The minimal error of [Chl] estimation by both the NN and PLS models was higher than that of $CI_{red\ edge}$ and was achieved using all seven spectral bands (CV = 13.53%); using only three bands, 540–580, 732.5–747.5, and 770–780 nm, allowed for accurate estimation of Chl with CV = 13.63%.

$CRI_{red\ edge}$ employing bands centered at 490, 705, and 783 nm was able to estimate Car content with CV below 27%. CV was a little bit higher (28.5%) when the band at 705 nm was replaced by the band at 740 nm. Car estimation by NN and PLS was more accurate than that by $CRI_{red\ edge}$ (Table 5.3). *The highest accuracy (CV = 19.6%) was achieved using four spectral bands (B2, B4, B6, B7) in the blue, red, red edge, and NIR ranges of the spectrum.* The CV of [Car] estimation using MSI bands was about 3%–4% higher than that using 20-nm-wide optimal bands. This is likely due to the use of the band B2 positioned in the green edge region between 460 and 525 nm. The width of this band does not correspond to the required 10–15-nm width of the band positioned at 510 nm, where maximal sensitivity of reflectance to [Car] content was found [30,34,60].

While green and red edge CI were tested at close range at the canopy level [62] as well as using TM Landsat data [63], the Car and AnC models were not tested at the canopy level. It is also necessary to examine the presented techniques at other scales. For now, it remains unclear whether the found linear relationships between the models and pigment content also hold on a coarser spatial scale. It has to be examined if the proposed techniques are able to estimate Car content at the canopy scale using airborne and satellite data, which is typically influenced by atmosphere, bidirectional reflectance distribution function effects, canopy shadows, and soil background.

5.6 CONCLUDING REMARKS

The progress in the technology achieved over the last decade enabled precise and quick assessment of key plant pigments, including Chl, Car, and AnC *in situ*. Successful application of this approach, based mostly on reflectance spectroscopy, depends on the correct selection of informative spectral bands, which might not be trivial, especially in the case of pigments with strongly overlapping absorption bands. Furthermore, the comparison of the relationships between absorbance and reflectance vs. pigment content in leaves using large data sets collected across plant species, developmental stages, and physiological states obviated certain limitations of reflectance-based quantification of the foliar pigments, especially in the blue and red, manifesting itself as a failure of linear correlation between reciprocal reflectance and absorbance. In terms of Kubelka-Munk theory describing the behavior of relatively weak absorbers evenly distributed in a thick layer of a highly reflective substance

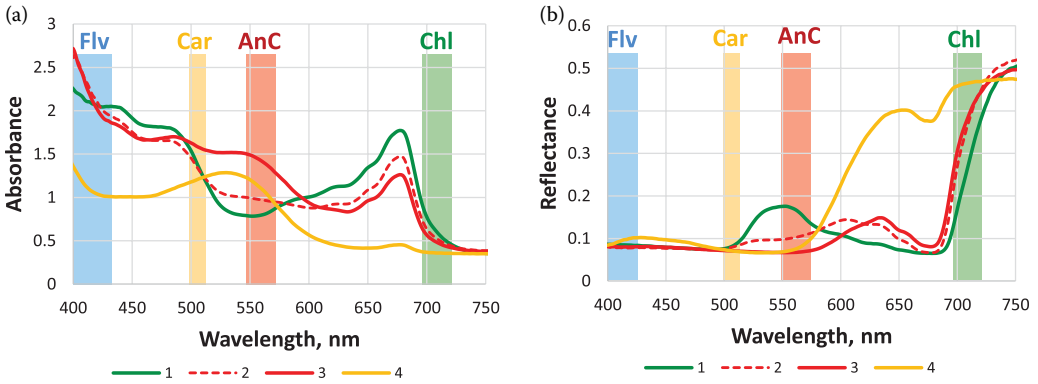

FIGURE 5.18 Absorbance and reflectance spectra of four Virginia creeper leaves with variable Chl, Car, AnC, and Flv contents (Table 5.5). Shaded areas represent spectral ranges found to be optimal for estimating pigment contents: [Chl]—green, model presented in the Equation 5.5; [AnC]—red, model presented in the Equation 5.11; [Car]—yellow, model presented in the Equation 5.8; and [Flv]—blue, model presented in the Equation 5.12. In models presented in the Equations 5.5 and 5.8, the 770–800 nm NIR range has been used.

[27], these limitations stem from (i) large extinction coefficients of Chl and other pigments [42], (ii) their high content in and (iii) structural complexity of the leaf and its photosynthetic apparatus [43]. Another plausible reason is backscattering from the superficial structures of plants such as leaf cuticle [44] contributing to the total leaf reflectance, especially in the blue, but bearing little or no information about the photosynthetic pigment composition of the leaf, hence decreasing the "information payload" of the total reflected signal.

In view of these difficulties, the reflectance-based approach is feasible only in certain spectral ranges positioned outside the main absorption bands of the pigments, mainly in the long-wave part of the visible range, red edge, and NIR [33,34]. To support the informed selection of suitable spectral bands for application of reflectance-based techniques, we proposed criteria, the traits $R\alpha$ and $R\rho^{-1}$, as quantitative measures of the α and ρ^{-1} responses to content of the pigment of interest. Importantly, spectral responses $R\alpha$ and $R\rho^{-1}$ complement specific optical properties, revealing the quantitative effect of each pigment on the background of other pigment absorption on α and ρ^{-1}.

The spectral bands selected based on these criteria are in line with the results of previous studies [19,34,45,46]. The task of spectral band selection can be further simplified by the elimination of useless spectral channels as outlined above, and the reduced set of spectral bands can be employed in different (NN-, PLS-, and VI-based) models for pigment content estimation. All three models were found to provide accurate estimations of foliar Chl content across three tree species. The Chl index using only two spectral bands in the red edge and NIR may be recommended for Chl estimation. NN and PLS with four spectral bands were the best for estimating carotenoid content; the NN model showed the highest accuracy. No techniques tested were species specific, allowing for estimating pigment content in different species without reparameterization of the model. All three

TABLE 5.5
Pigment Content (in μg/cm²) in Four Leaves Presented in Figure 5.18

Leaf	Chl	Car	AnC	Flv*10⁻¹
1	38	9.7	0.14	27.1
2	18.5	5.3	14	30.2
3	13	6.3	46	24.7
4	0.4	0.7	40	10.4

techniques performed consistently well and yielded accurate estimations of pigment content when spectral bands were simulated in accord with the spectral response of the multispectral instrument on the Sentinel-2 satellite.

As a more generic approach capable of overcoming the limitations of reflectance-based models, we introduced the concept of specific absorbance response, objectively showing the contribution of each pigment group to light absorption, and deduced the *in situ* absorbance of foliar Chl, Car, AnC, and Flv, obviously free from the limitations typical of reflectance-based approaches. The absorbance-based algorithms demonstrated increased dynamic range and linear relationships with the leaf pigment content, especially pronounced in the shortwave part of the visible spectrum.

Based on the comparative account of advantages and drawbacks of reflectance- and absorbance-based pigment estimation, we argue that these approaches complement each other and can be used synergistically in advanced models for precision estimation of foliar pigments. We believe that the "response traits" are very instructive for understanding the *combined effect of pigments* on optical properties, which is at the foundation of knowledge-driven selection of spectral bands for creating new and improving existing models for noninvasive remote estimation of pigments.

The recently developed PROSPECT-D model includes, for the first time, the three main leaf pigments as independent constituents: Chl, Car, and AnC [43]. PROSPECT-D was tested on several data sets displaying many plant species with a large range of leaf traits and pigment composition, and showed very accurate estimation of Chl, Car, and AnC using hyperspectral transmittance and reflectance data. The accuracy of Chl estimation by the red edge Chl index ($CI_{red\ edge}$) was slightly better than that of Prospect D (4.5% vs. 5.5%), while the accuracy of AnC estimation by ARI (6.1%) and mARI (6.4%) was significantly better than that of Prospect D (9.5%). Significantly, Prospect D probably provides the only way to accurately estimate Car content in AnC-containing leaves [13]. Thus, the application of both data-driven and radiative transfer modeling are alternatives for developing generic algorithms estimating the content of all pigment groups. The combination of the two approaches brought desirable alternatives to extensive data collection (mandatory for the former) and high computational resources required by the latter [64,65].

Combining the approaches presented in this chapter, one can dramatically improve noninvasive estimation of the pigments absorbed in blue (flavonoids) and blue-green (carotenoids) on the background of strong overlapping absorption of other pigments. It is essential not only for those involved in remote estimation of pigments per se, but for plant biologists as well. Thus, our findings provide for a better understanding of light interaction with leaves, which translates into a deeper insight into the *in-situ* light absorption properties of all key plant pigment groups. This approach will constitute a handy tool for plant physiologists and photobiologists for dissecting the environmental stress effects in plants, especially for comparative analysis of interception of light by photosynthetic and photoprotective pigments as a function of physiological condition and developmental stage.

ACKNOWLEDGMENTS

This chapter is dedicated to late Mark N. Merzlyak, an extremely bright and productive scholar. He worked in many fields of biology and physiology. In each of them, his contributions were among the highest. Among others were free-radical oxidation of lipids, syndrome of lipid peroxidation in plants, phytoimmunology, and stress- and senescence-induced degradation of plant pigments. He contributed enormously in leaf optics and development techniques for foliar pigment retrieval. He was the best friend and we miss him tremendously.

We acknowledge the contributions of Drs. Veronica Ciganda, Robi Stark, Mark Steele, Andres Vina, and Yoav Zur. We are grateful to our colleagues Drs. Claus Buschmann, Olga B. Chivkunova, Harmut Lichtenthaler, and Donald C. Rundquist for helping us at different stages of this study. The support of Center for Advanced Land Management and Information Technologies at University of Nebraska, J. Blaustein Institute for Desert Research of Ben-Gurion University, Israel, and the Russian Science Foundation (to AS, grant 14–50-00029) is greatly appreciated.

REFERENCES

1. N. Liguori, X. Periole, S.J. Marrink, R. Croce, From light-harvesting to photoprotection: Structural basis of the dynamic switch of the major antenna complex of plants (LHCII), *Scientific Reports*, 5: 2015, 15661.
2. A.N. Tikhonov, A.V. Vershubskii, Computer modeling of electron and proton transport in chloroplasts, *Biosystems*, 121: 2014, 1–21.
3. R. Croce, H. van Amerongen, Natural strategies for photosynthetic light harvesting, *Nature Chemical Biology*, 10: 2014, 492–501.
4. B. Demmig-Adams, C. Cohu, O. Muller, W. Adams, III, Modulation of photosynthetic energy conversion efficiency in nature: From seconds to seasons, *Photosynthesis Research*, 113: 2012, 75–88.
5. P. Horton, Developments in research on non-photochemical fluorescence quenching: Emergence of key ideas, theories and experimental approaches, in: B. Demmig-Adams, G. Garab, W. Adams Iii, Govindjee (Eds.) *Non-Photochemical Quenching and Energy Dissipation in Plants, Algae and Cyanobacteria*, Springer, Netherlands, Dordrecht, 2014, pp. 73–95.
6. G. Giuliano, Plant carotenoids: Genomics meets multi-gene engineering, *Current Opinion in Plant Biology*, 19: 2014, 111–117.
7. A. Solovchenko, K. Neverov, Carotenogenic response in photosynthetic organisms: A colorful story, *Photosynthesis Research*, 2017.
8. M.N. Merzlyak, A.E. Solovchenko, Photostability of pigments in ripening apple fruit: A possible photoprotective role of carotenoids during plant senescence, *Plant Science*, 163: 2002, 881–888.
9. M. Merzlyak, A. Gitelson, O. Chivkunova, V. Rakitin, Non-destructive optical detection of pigment changes during leaf senescence and fruit ripening, *Plant Physiol*, 106: 1999, 135–141.
10. B. Winkel-Shirley, Flavonoid biosynthesis. A colorful model for genetics, biochemistry, cell biology, and biotechnology, *Am Soc Plant Biol*, 2001, 485–493.
11. N. Hughes, C. Morley, W. Smith, Coordination of anthocyanin decline and photosynthetic maturation in juvenile leaves of three deciduous tree species, *New Phytologist*, 175: 2007, 675–685.
12. G. Agati, C. Brunetti, M. Di Ferdinando, F. Ferrini, S. Pollastri, M. Tattini, Functional roles of flavonoids in photoprotection: New evidence, lessons from the past, *Plant Physiology and Biochemistry*, 72: 2013, 35–45.
13. M.N. Merzlyak, O.B. Chivkunova, A.E. Solovchenko, K.R. Naqvi, Light absorption by anthocyanins in juvenile, stressed, and senescing leaves, *Journal of Experimental Botany*, 59: 2008, 3903–3911.
14. B. Winkel-Shirley, Biosynthesis of flavonoids and effects of stress, *Current Opinion in Plant Biology*, 5: 2002, 218–223.
15. J.-H.B. Hatier, K.S. Gould, *Anthocyanin Function in Vegetative Organs, Anthocyanins*, Springer Science+Business Media, New York, NY, 2009, pp. 1–19.
16. K. Gould, Nature's Swiss army knife: The diverse protective roles of anthocyanins in leaves, *Journal of Biomedicine and Biotechnology*, 5: 2004, 314–320.
17. D. Strack, T. Vogt, W. Schliemann, Recent advances in betalain research, *Phytochemistry*, 62: 2003, 247–269.
18. Y. Tanaka, N. Sasaki, A. Ohmiya, Biosynthesis of plant pigments: Anthocyanins, betalains and carotenoids, *Plant Journal*, 54: 2008, 733.
19. A. Richardson, S. Duigan, G. Berlyn, An evaluation of noninvasive methods to estimate foliar chlorophyll content, *New Phytologist*, 2002, 185–194.
20. M.F. Garbulsky, J. Peñuelas, J. Gamon, Y. Inoue, I. Filella, The photochemical reflectance index (PRI) and the remote sensing of leaf, canopy and ecosystem radiation use efficiencies: A review and meta-analysis, *Remote Sensing of Environment*, 115: 2011, 281–297.
21. P.J. Curran, J.L. Dungan, H.L. Gholz, Exploring the relationship between reflectance red edge and chlorophyll content in slash pine, *Tree Physiology*, 7: 1990, 33–48.
22. I. Filella, L. Serrano, J. Serra, J. Penuelas, Evaluating wheat nitrogen status with canopy reflectance indices and discriminant analysis, *Crop Science*, 35: 1995, 1400–1405.
23. M. Schlemmer, A. Gitelson, J. Schepers, R. Ferguson, Y. Peng, J. Shanahan, D. Rundquist, Remote estimation of nitrogen and chlorophyll contents in maize at leaf and canopy levels, *International Journal of Applied Earth Observation and Geoinformation*, 25: 2013, 47–54.
24. H.K. Lichtenthaler, A. Ac, M.V. Marek, J. Kalina, O. Urban, Differences in pigment composition, photosynthetic rates and chlorophyll fluorescence images of sun and shade leaves of four tree species, *Plant Physiol Biochem*, 45: 2007, 577–588.
25. J. Cavender-Bares, J.A. Gamon, S.E. Hobbie, M.D. Madritch, J.E. Meireles, A.K. Schweiger, P.A. Townsend, Harnessing plant spectra to integrate the biodiversity sciences across biological and spatial scales, *Am J Bot*, 2017.

26. S.L. Ustin, J.A. Gamon, Remote sensing of plant functional types, *New Phytologist*, 186: 2010, 795–816.
27. G. Kortüm, *Reflectance Spectroscopy: Principles, Methods, Applications*, Springer, New York, 1969.
28. R. Kumar, L. Silva, Light ray tracing through a leaf cross section, *Applied Optics*, 12: 1973, 2950–2954.
29. A. Gitelson, Y. Gritz, M. Merzlyak, Non destructive chlorophyll assessment in higher plant leaves: Algorithms and accuracy, *Journal of Plant Physiology*, 160: 2003, 271–282.
30. E. Chappelle, M. Kim, J. McMurtrey III, Ratio analysis of reflectance spectra (RARS): An algorithm for the remote estimation of the concentrations of chlorophyll *a*, chlorophyll *b*, and carotenoids in soybean leaves, *Remote Sensing of Environment*, 39: 1992, 239–247.
31. J. Gamon, J. Penuelas, C. Field, A narrow-waveband spectral index that tracks diurnal changes in photosynthetic efficiency, *Remote Sensing of Environment*, 41: 1992, 35–44.
32. G. Blackburn, Quantifying chlorophylls and carotenoids at leaf and canopy scales: An evaluation of some hyperspectral approaches, *Remote Sensing of Environment*, 66: 1998, 273–285.
33. J. Gamon, J. Surfus, Assessing leaf pigment content and activity with a reflectometer, *The New Phytologist*, 143: 1999, 105–117.
34. A. Gitelson, G. Keydan, M. Merzlyak, Three-band model for noninvasive estimation of chlorophyll, carotenoids, and anthocyanin contents in higher plant leaves, *Geophysical Research Letters*, 33: 2006, L11402.
35. A. Gitelson, O. Chivkunova, T. Zhigalova, A. Solovchenko, *In situ* optical properties of foliar flavonoids: Implication for non-destructive estimation of flavonoid content, *Journal of Plant Physiology*, 218: 2017, 258–264.
36. S. Jacquemoud, S. Ustin, Application of radiative transfer models to moisture content estimation and burned land mapping, *4th International Workshop on Remote Sensing and GIS Applications to Forest Fire Management*, 2003.
37. O. Kira, R. Linker, A. Gitelson, Non-destructive estimation of foliar chlorophyll and carotenoid contents: Focus on informative spectral bands, *International Journal of Applied Earth Observation and Geoinformation*, 38: 2015, 251–260.
38. C. Buschmann, E. Nagel, *In vivo* spectroscopy and internal optics of leaves as basis for remote sensing of vegetation, *International Journal of Remote Sensing*, 14: 1993, 711–722.
39. A. Gitelson, M. Merzlyak, Quantitative estimation of chlorophyll-*a* using reflectance spectra: Experiments with autumn chestnut and maple leaves, *Journal of Photochemistry and Photobiology. B, Biology*, 22: 1994, 247–252.
40. A.A. Gitelson, M.N. Merzlyak, O.B. Chivkunova, Optical properties and nondestructive estimation of anthocyanin content in plant leaves, *Photochem Photobiol*, 74: 2001, 38–45.
41. M. Steele, A. Gitelson, D. Rundquist, M. Merzlyak, Nondestructive estimation of anthocyanin content in grapevine leaves, *American Journal of Enology and Viticulture*, 60: 2009, 87–92.
42. H. Lichtenthaler, Chlorophyll and carotenoids: Pigments of photosynthetic biomembranes, *Methods of Enzymology*, 1987, 331–382.
43. J.B. Féret, A.A. Gitelson, S.D. Noble, S. Jacquemoud, PROSPECT-D: Towards modeling leaf optical properties through a complete lifecycle, *Remote Sensing of Environment*, 193: 2017, 204–215.
44. P. Baur, K. Stulle, B. Uhlig, J. Schönherr, Absorption von strahlung im UV-B und blaulichtbereich von blattkutikeln ausgewählter nutzpflanzen, *Gartenbauwissenschaft*, 63: 1998, 145–152.
45. O. Kira, A.L. Nguy-Robertson, T.J. Arkebauer, R. Linker, A.A. Gitelson, Informative spectral bands for remote green LAI estimation in C3 and C4 crops, *Agricultural and Forest Meteorology*, 218: 2016, 243–249.
46. S.L. Ustin, A.A. Gitelson, S. Jacquemoud, M. Schaepman, G.P. Asner, J.A. Gamon, P. Zarco-Tejada, Retrieval of foliar information about plant pigment systems from high resolution spectroscopy, *Remote Sensing of Environment*, 113: 2009, S67–S77.
47. M.N. Merzlyak, O.B. Chivkunova, T.B. Melo, K.R. Naqvi, Does a leaf absorb radiation in the near infrared (780-900 nm) region? A new approach to quantifying optical reflection, absorption and transmission of leaves, *Photosynth Res*, 72: 2002, 263–270.
48. A.A. Gitelson, J.A. Gamon, A. Solovchenko, Multiple drivers of seasonal change in PRI: Implications for photosynthesis 1. *Leaf Level, Remote Sensing of Environment*, 191: 2017, 110–116.
49. F.E. Fassnacht, S. Stenzel, A.A. Gitelson, Non-destructive estimation of foliar carotenoid content of tree species using merged vegetation indices, *Journal of Plant Physiology*, 176: 2015, 210–217.
50. A. Palacios-Orueta, S. Khanna, J. Litago, M.L. Whiting, S.L. Ustin, Assessment of NDVI and NDWI spectral indices using MODIS time series analysis and development of a new spectral index based on MODIS shortwave infrared bands, *Proceedings of the 1st International Conference of Remote Sensing and Geoinformation Processing*, Trier, Germany. http://ubt.opus.hbz-nrw.de/volltexte/2006/362/pdf/03-rgldd-session2.pdf, 2006, pp. 207–209.

51. S. Khanna, A. Palacios-Orueta, M.L. Whiting, S.L. Ustin, D. Riaño, J. Litago, Development of angle indexes for soil moisture estimation, dry matter detection and land-cover discrimination, *Remote Sensing of Environment*, 109: 2007, 154–165.
52. V. Centner, D.-L. Massart, O.E. de Noord, S. de Jong, B.M. Vandeginste, C. Sterna, Elimination of uninformative variables for multivariate calibration, *Analytical Chemistry*, 68: 1996, 3851–3858.
53. A. Gitelson, M. Merzlyak, Signature analysis of leaf reflectance spectra: Algorithm development for remote sensing of chlorophyll, *Journal of Plant Physiology*, 148: 1996, 494–500.
54. H. Gausman, W. Allen, R. Cardenas, Reflectance of cotton leaves and their structure, *Remote Sensing of Environment*, 1: 1969, 19–22.
55. L. Fukshansky, A. Remisowsky, J. McClendon, A. Ritterbusch, T. Richter, H. Mohr, Absorption spectra of leaves corrected for scattering and distributional error: A radiative transfer and absorption statistics treatment, *Photochemistry and Photobiology*, 57: 1993, 538–555.
56. M. Merzlyak, A. Gitelson, Why and what for the leaves are yellow in autumn? On the interpretation of optical spectra of senescing leaves(*Acer platanoides* L.), *Journal of Plant Physiology*, 145: 1995, 315–320.
57. G. Le Maire, C. Francois, E. Dufrene, Towards universal broad leaf chlorophyll indices using PROSPECT simulated database and hyperspectral reflectance measurements, *Remote Sensing of Environment*, 89: 2004, 1–28.
58. J.G. Clevers, A.A. Gitelson, Remote estimation of crop and grass chlorophyll and nitrogen content using red-edge bands on Sentinel-2 and-3, *International Journal of Applied Earth Observation and Geoinformation*, 23: 2013, 344–351.
59. D. Sims, J. Gamon, Relationship between leaf pigment content and spectral reflectance across a wide range species, leaf structures and development stages, *Remote Sensing of Environment*, 81: 2002, 351–354.
60. A. Gitelson, Y. Zur, O. Chivkunova, M. Merzlyak, Assessing carotenoid content in plant leaves with reflectance spectroscopy, *Photochem Photobiol*, 75: 2002, 272–281.
61. Y. Grossman, S. Ustin, S. Jacquemoud, E. Sanderson, G. Schmuck, J. Verdebout, Critique of stepwise multiple linear regression for the extraction of leaf biochemistry information from leaf reflectance data, *Remote Sensing of Environment*, 56: 1996, 182–193.
62. A. Gitelson, S. Laorawat, G. Keydan, A. Vonshak, Optical properties of dense algal cultures outdoors and their application to remote estimation of biomass and pigment concentration in *Spirulina platensis* (Cyanobacteria), *Journal of Phycology*, 31: 1995, 828–834.
63. C. Wu, L. Wang, Z. Niu, S. Gao, M. Wu, Nondestructive estimation of canopy chlorophyll content using Hyperion and Landsat/TM images, *International Journal of Remote Sensing*, 31: 2010, 2159–2167.
64. J.-B. Féret, C. François, A. Gitelson, G.P. Asner, K.M. Barry, C. Panigada, A.D. Richardson, S. Jacquemoud, Optimizing spectral indices and chemometric analysis of leaf chemical properties using radiative transfer modeling, *Remote Sensing of Environment*, 115: 2011, 2742–2750.
65. J. Verrelst, G. Camps-Valls, J. Muñoz-Marí, J.P. Rivera, F. Veroustraete, J.G. Clevers, J. Moreno, Optical remote sensing and the retrieval of terrestrial vegetation bio-geophysical properties—A review, *ISPRS Journal of Photogrammetry and Remote Sensing*, 108: 2015, 273–290.
66. A. Gitelson, A. Solovchenko, Generic algorithms for estimating foliar pigment content, *Geophysical Research Letters*, 2017.